Sampled-data extremum-seeking framework for constrained optimization of nonlinear dynamical systems

Automatica 142 (2022) 110415

Contents lists available at ScienceDirect

Automatica

journal homepage: www.elsevier.com/locate/automatica

Sampled-data extremum-seeking framework for constrained optimization of nonlinear dynamical systems ☆

Leroy Hazeleger [a,*], Dragan Nešić [b], Nathan van de Wouw [a,c]

[a] Eindhoven University of Technology, Department of Mechanical Engineering, Eindhoven 5600 MB, The Netherlands
[b] The University of Melbourne, Department of Electrical and Electronic Engineering, Melbourne, VIC 3010, Australia
[c] University of Minnesota, Department of Civil, Environmental and Geo-Engineering, Minneapolis, MN 55455, USA

ARTICLE INFO

Article history:
Received 19 June 2020
Received in revised form 21 December 2021
Accepted 19 April 2022
Available online 31 May 2022

Keywords:
Sampled-data systems
Extremum-seeking control
Constrained optimization

ABSTRACT

Most extremum-seeking control (ESC) approaches focus solely on the problem of finding the extremum of some unknown, steady-state input–output map, providing parameter settings that lead to optimal steady-state system performance. However, many industrial applications also have to deal with constraints on operating conditions due to, e.g., actuator limitations, limitations on tunable system parameters, or constraints on measurable variables. In particular, constraints on measurable variables are typically unknown in terms of their relationship with the tunable system parameters. In addition, the constraints on system inputs as a result of the constraints on measurable variables may conflict with the otherwise optimal operational condition, and hence should be taken into account in the data-based optimization approach. In this work, we propose a sampled-data extremum-seeking framework for the constrained optimization of a class of nonlinear dynamical systems with measurable constrained variables. In this framework, barrier function methods are employed, exploiting both the objective function and constraint functions which are available through output measurement only. We show, under the assumption that the parametric initialization yield operating conditions that do not violate the constraints, that (1) the resulting closed-loop dynamics is stable, (2) constraint satisfaction of the inputs is guaranteed for all iterations of the optimization process, and (3) constrained optimization is achieved. We illustrate the working principle of the proposed framework by means of an industrial case study of the constrained optimization of extreme ultraviolet light generation in a laser-produced plasma source within a state-of-the-art lithography system.

1. Introduction

Performance optimization of complex nonlinear dynamical systems is a challenging task. Namely, most (numerical) optimization techniques such as, e.g., gradient-descent methods, Newton and quasi-Newton methods, interior-point methods, and Sequential Quadratic Programming (SQP), usually rely on an accurate model of the process to be optimized (Boyd & Vandenberghe, 2009), while such a model can be hard or impossible to obtain for complex nonlinear systems. Nevertheless, the steady-state input–output behavior of many of such systems possesses optimal performance under particular operating conditions and we often desire to find such optimal operating conditions. Based solely on output measurements and without using any model knowledge, *extremum-seeking control* (ESC) is able to optimize the performance of such complex systems in real-time by adjusting these operating conditions and driving the system into a neighborhood of its optimal steady-state input–output behavior (Krstić & Wang, 2000; Teel & Popović, 2001).

Along with the pioneering work done in Krstić and Wang (2000) on convergence proofs for continuous-time extremum-seeking schemes based on sinusoidal perturbations, a notable contribution to the field of extremum-seeking control was made in Teel and Popović (2001). In Teel and Popović (2001), it was shown that under assumptions on the asymptotic stability of both the system and on a discrete-time nonlinear programming method used for optimization, extremum seeking can be achieved within a periodic sampled-data framework. This framework allows the use of a wide class of smooth and nonsmooth optimization algorithms for achieving optimization of general nonlinear

☆ This work is part of the research programme CHAMeleon with project number 13896, which is (partly) financed by the Netherlands Organisation for Scientific Research (NWO), The Netherlands. The material in this paper was partially presented at the 58th IEEE Conference on Decision and Control, December 11–13, 2019, Nice, France. This paper was recommended for publication in revised form by Associate Editor Debasish Chatterjee under the direction of Editor Daniel Liberzon.

* Corresponding author.
E-mail addresses: leroy.hazeleger@thermofisher.com (L. Hazeleger), dnesic@unimelb.edu.au (D. Nešić), n.v.d.wouw@tue.nl (N. van de Wouw).

https://doi.org/10.1016/j.automatica.2022.110415

systems. In Kvaternik and Pavel (2011), closed-loop stability of the sampled-data ESC scheme has been studied from an interconnected systems' theory point-of-view, in which stability results are obtained by imposing stronger conditions on the nonlinear programming methods than done in Teel and Popović (2001).

Extensions of the framework in Teel and Popović (2001) are provided in Khong, Nešić, Tan, and Manzie (2013a, 2013b). The work in Khong et al. (2013a) utilizes a trajectory-based approach to prove semi-global practical asymptotic stability of the proposed sampled-data extremum-seeking schemes as opposed to the Lyapunov-type arguments used in Teel and Popović (2001). The former exploits the notion of multi-step consistency (see, e.g., Nešić, Teel, & Kokotović, 1999) while the latter exploits closeness of solutions of a differential inclusion over a single time step. As such, the framework in Khong et al. (2013a) allows to use a broader class of optimization algorithms, including algorithms which do not admit a state-update realization and/or Lyapunov function. Subsequently in Khong et al. (2013b), the framework in Khong et al. (2013a) was extended to a more generic framework, which in addition to gradient-based optimization algorithms, also encompasses sampling-based (global) optimization methods capable of non-convex optimization, enabling extremum seeking for an even wider class of problems. For example, in Khong, Nešić, Manzie and Tan (2013) and Nešić, Nguyen, Tan, and Manzie (2013), two sampling-based algorithms are presented that are able to achieve (a weaker type of) convergence to a global optimum.

Most extremum-seeking approaches, whether it is of the continuous-time type as in Krstić and Wang (2000) or the sampled-data type as in Khong et al. (2013a) and Teel and Popović (2001), focus solely on the problem of finding the extremum of some unknown steady-state input–output map, providing parameter settings that lead to optimal steady-state system performance. However, many industrial applications also have to deal with constraints on operating conditions due to, e.g., actuator limitations, limitations on design or tunable system parameters, or constraints on measurable signals. The constraints on system inputs as a result of measurable constrained variables may conflict with the otherwise optimal operational condition, and hence should be taken into account in the data-based optimization approach.

In terms of dealing with constraints in extremum-seeking schemes, existing approaches can be divided into two main categories: (i) approaches that assume a-priori knowledge on constrained operating conditions in the form of explicit constraint functions, and (ii) approaches that deal with *unknown* but *measurable constraint functions*. Extremum-seeking approaches that explicitly deal with known constraint functions are considered in, e.g., DeHaan and Guay (2005), Mills and Krstić (2014) and Tan, Li, and Mareels (2013). In DeHaan and Guay (2005) and Tan et al. (2013), penalty/barrier functions are employed to adapt the search space so as not to violate the constraints. Another approach proposed in Tan et al. (2013) employs an anti-windup scheme to prevent the optimizer from leaving the known admissible search space. In Mills and Krstić (2014), constraint satisfaction is achieved by employing a projection operator in the extremum-seeking scheme. Although not aimed at constrained optimization, the sampling-based algorithms in Khong, Nešić, Manzie et al. (2013) and Nešić et al. (2013) operate in an a-priori defined compact (input) set, i.e., these allow incorporation of *known* (input) constraints to adjust the search space.

Extremum-seeking approaches for (strictly) convex optimization problems with unknown but measurable constraint functions are considered in, e.g., Atta, Guay, and Lucchese (2019), Dürr, Zeng, and Ebenbauer (2013), Guay, Moshksar, and Dochain (2014), Labar, Garone, Kinnaert, and Ebenbauer (2019), Liao, Manzie, Chapman, and Alpcan (2019), Ramos, Manzie, and Shekhar (2017), Srinivasan, Biegler, and Bonvin (2008) and van der Weijst, van Keulen, and Willems (2019), albeit in the continuous-time extremum-seeking setting. In Guay et al. (2014), Labar et al. (2019) and Srinivasan et al. (2008), a combined barrier/penalty function approach is employed to transform the constrained optimization problem into an unconstrained problem using an augmented cost. The methods allow small violations of the constraints (during transients) to avoid difficulties in practical applications, e.g., due to the presence of uncertainty and disturbances, or to relax the choice of initial, possibly inadmissible, inputs. Optimization is accomplished by estimation of the gradient of the augmented cost and a gradient-based optimization algorithm. In Dürr et al. (2013), a combination of the classical extremum-seeking approach as in Krstić and Wang (2000) and so-called saddle point algorithms as in Dürr and Ebenbauer (2011) are used to find the constrained minimizer. In Atta et al. (2019), Liao et al. (2019), Ramos et al. (2017), and van der Weijst et al. (2019), gradient-based extremum-seeking approaches are employed that combines the gradients of the objective function and the constraint functions to deal with measurable constraints. In Liao et al. (2019), Ramos et al. (2017), and van der Weijst et al. (2019) a so-called transition function is designed that enables a gradient-based optimizer to switch smoothly between the gradient of the to-be-optimized objective function, typically when constraints are not violated, and the gradient of the constraint functions when the constraints are violated. In Atta et al. (2019), a projection operator is employed that finds a feasible direction without constraint violation.

In this work, we focus on sampled-data extremum-seeking schemes as in Teel and Popović (2001), as opposed to continuous-time extremum-seeking schemes as in Krstić and Wang (2000). Namely, sampled-data schemes are compelling given the potential of including diverse types of optimization algorithms, see, e.g., Khong et al. (2013b), Teel (2000a, 2000b) and Teel and Popović (2001). Here, we extend the class of optimization algorithms in Teel and Popović (2001) to a class of constrained optimization algorithms to achieve extremum-seeking in the presence of unknown but measurable constraints by employing barrier function methods. Moreover, we solve the problem of finding optimal system inputs for which (steady-state) constraint satisfaction can only be assessed on the basis of measurable constraint functions.

The main contributions of this work can be summarized as follows. First, we extend the class of optimization problems as studied in Teel and Popović (2001) to a class of constrained optimization problems, for which we consider a class of dynamical systems where both a to-be-optimized objective function and constraint functions are available through measurement only. Second, we extend the class of smooth and nonsmooth optimization algorithms to facilitate extremum-seeking in the presence of unknown but measurable constraints by employing barrier function methods. Third, under the assumption that the parametric initialization yield operating conditions that do not violate the constraints on measurable constraint functions in steady-state, we (1) prove closed-loop stability of the interconnection between the class of dynamical systems and the proposed class of constrained optimization algorithms, (2) show strict constraint satisfaction of the inputs for all iterations of the optimization process, and (3) constrained optimization is achieved. Fourth, we illustrate the working principle of the proposed framework by means of a representative industrial case study of the constrained optimization of extreme ultraviolet (EUV) light generation in a laser produced plasma (LPP) source within a state-of-the-art lithography system.

Preliminary results of this work were published in Hazeleger, Nešić, and van de Wouw (2019), which extends the sampled-data

extremum-seeking framework as studied in Kvaternik and Pavel (2011). The work in Hazeleger et al. (2019) facilitates extremum-seeking for constrained optimization of dynamical systems using barrier function methods, albeit for a limited class of systems, and under more stringent conditions on the class of algorithms. Moreover, only an academic numerical example is provided. In the current work, a more general class of dynamical systems and class of algorithms are considered than the ones considered in Hazeleger et al. (2019), and the conditions on the class of algorithms are milder. In addition, this work contains an illustrative industrial case study.

The paper is organized as follows. Section 2 presents the class of dynamical systems and the constrained optimization problem formulation. Section 3 presents the class of extremum seeking algorithms to facilitate constrained optimization. In Section 4, a closed-loop stability analysis is provided. Section 5 presents the industrial case study. Section 6 closes with conclusions.

We use the following notations:

- A function $\gamma : \mathbb{R}_{\geq 0} \to \mathbb{R}_{\geq 0}$ is of class $\mathcal{K}$ (denoted as $\gamma \in \mathcal{K}$) if it is continuous, strictly increasing, and $\gamma(0) = 0$. If γ is also unbounded, then $\gamma \in \mathcal{K}_\infty$.
- A continuous function $\beta : \mathbb{R}_{\geq 0} \times \mathbb{R}_{\geq 0} \to \mathbb{R}_{\geq 0}$ is of class $\mathcal{KL}$, if, for each fixed t, $\beta(\cdot, t) \in \mathcal{K}$ and, for each s, $\beta(s, \cdot)$ is decreasing to zero.
- Let $\mathcal{X}$ be a Banach space whose norm is denoted by $\|\cdot\|$. Given any subset $\mathcal{Y}$ of $\mathcal{X}$, i.e. $\mathcal{Y} \subset \mathcal{X}$, and a point $x \in \mathcal{X}$, the distance of x from $\mathcal{Y}$ is defined as $\|x\|_{\mathcal{Y}} := \inf_{a \in \mathcal{Y}} \|x - a\|$.
- $\mathcal{A} + \epsilon\bar{\mathcal{B}}$ is an ϵ-neighborhood of $\mathcal{A}$, and $\bar{\mathcal{B}}$ can be identified with the closed unit ball.
- We use the following simplified notation for discrete systems, e.g., $u_{k+1} \in F(u_k) \to u^+ \in F(u)$.
- Let $\lfloor \cdot \rfloor$ denote the floor operator.
- The function $\mathrm{id}(\cdot)$ denotes the identity function.

2. Class of dynamical systems and constrained optimization problem formulation

In this section, we introduce the class of nonlinear, possibly infinite-dimensional, systems having multiple measurable outputs. In particular, we consider system outputs that are related to (1) a measurable (to-be-optimized) cost and (2) measurable constrained variables. Depending on the output constraints at hand, parameter settings that optimize the measurable cost may not satisfy the output constraints. Therefore, this section introduces the constrained optimization problem for that class of systems.

2.1. Class of dynamical systems

The following definition of the class of systems is based on the ones from Khong et al. (2013b) and Teel and Popović (2001).

Definition 1. The dynamical system Σ_p is time-invariant, with state $x \in \mathcal{X}$, where $\mathcal{X}$ is a Banach space with norm $\|\cdot\|$. The input to the system is denoted by $u \in \mathbb{R}^{n_u}$. We consider the system to have $n_z + 1$ measurable outputs, separated into two channels, denoted by $y \in \mathbb{R}$, and $z \in \mathbb{R}^{n_z}$, and referred to as the cost output and the constraint outputs, respectively. Given any constant input $u \in \mathbb{R}^{n_u}$ and initial state $x_0 \in \mathcal{X}$, let $x(\cdot, x_0, u)$ be the state trajectory of the dynamical system Σ_p starting at x_0 with input u. Let $\mathcal{S}(x_0, u)$ be the set of all possible trajectories starting at x_0 and with constant input u.

In the context of ESC, Σ_p in Definition 1 represents the dynamical system to-be optimized, where the input u can be regarded as a vector of tunable system parameters, and the outputs y and z can be regarded as a measurable performance variable and a vector of measurable constrained variables, respectively. The following assumption states properties that the class of systems described in Definition 1 must possess, and is largely aligned with the assumptions in Khong et al. (2013b, Assumption 2) and Teel and Popović (2001, Assumption 1).

Assumption 2. Given a dynamical system Σ_p described by Definition 1, we assume that the following properties hold:

- For each constant input u the system's trajectory converges to a uniquely defined attractor, i.e., for each constant input $u \in \mathcal{T} \subseteq \mathbb{R}^{n_u}$, with $\mathcal{T}$ a nonempty (and possibly unknown) set, there exists only one, closed and nonempty set $\mathcal{A}(u) \subset \mathcal{X}$, such that
$$\lim_{t \to \infty} \|x(t, x_0, u)\|_{\mathcal{A}(u)} = 0. \tag{1}$$
This defines a set-valued mapping $\mathcal{A}(\cdot)$ from $\mathcal{T}$ to subsets of $\mathcal{X}$.
- There exist (unknown) continuous functions $h : \mathcal{X} \to \mathbb{R}$ and $g : \mathcal{X} \to \mathbb{R}^{n_z}$ that map the state evolution $x(\cdot, x_0, u)$ of the system, starting at $x_0 \in \mathcal{X}$ with constant input $u \in \mathcal{T}$, to the evolution of output channels y and z of the system, as follows:
$$\begin{aligned} y(t) &:= h(x(t, x_0, u)) \quad \forall\, t \geq 0, \\ z(t) &:= g(x(t, x_0, u)) \quad \forall\, t \geq 0, \end{aligned} \tag{2}$$
which are defined for any input $u \in \mathcal{T}$ and $x_0 \in \mathcal{X}$. Moreover, for any $x_1, x_2 \in \mathcal{A}(u)$, it is assumed that $h(x_1) = h(x_2)$ and $g(x_1) = g(x_2)$. Since the set-valued mapping $\mathcal{A}(u)$ is a uniquely defined attractor for any $x \in \mathcal{S}(x_0, u)$, and both h and g are continuous, for any constant $u \in \mathcal{T}$ and $x_0 \in \mathcal{X}$, we have that
$$\begin{aligned} Q(u) &:= \lim_{t \to \infty} h(x(t, x_0, u)), \\ G(u) &:= \lim_{t \to \infty} g(x(t, x_0, u)), \end{aligned} \tag{3}$$
which are well-defined (unknown) steady-state input–output maps on $\mathcal{T}$.
- We assume the (unknown) steady-state input–output mappings Q and G to be locally Lipschitz on $\mathcal{T}$.
- For any $\epsilon_1, \epsilon_2, \Delta_{x_0} \in \mathbb{R}_{>0}$, there exists a so-called waiting time $T > 0$ such that
$$\|x(t, x_0, u)\|_{\mathcal{A}(u)} \leq \epsilon_1 \|x_0\|_{\mathcal{A}(u)} + \epsilon_2, \tag{4}$$
for all $t \geq T$, all constant $u \in \mathcal{T}$, and all $\|x_0\|_{\mathcal{A}(u)} \leq \Delta_{x_0}$.

2.2. Constrained optimization problem formulation

The steady-state input–output mappings Q and G as defined in Assumption 2 represent the (unknown) steady-state cost function and the steady-state constraint functions of the plant Σ_p, respectively. Based on these steady-state input–output mappings, we can formulate the steady-state *constrained* optimization problem as follows:
$$\min_{u \in \mathcal{T}} \; Q(u) \text{ s.t. } G(u) \leq 0. \tag{5}$$
For the existence of a solution to the constrained optimization problem in (5) and the ability to find this solution, we adopt the following assumption.

Assumption 3. The nonempty (and possibly unknown) set $\mathcal{T}$ in Assumption 2 is defined as $\mathcal{T} := \{u \in \mathbb{R}^{n_u} \mid G(u) \leq 0\}$. We call the set $\mathcal{T}$ the *admissible set*. The steady-state input–output mapping Q takes its (global) constrained minimum value in a nonempty, compact set $\mathcal{C}_{\mathcal{T}} \subset \mathcal{T}$, i.e., there exist system inputs $u^* \in \mathcal{C}_{\mathcal{T}} \subset \mathcal{T}$ such that for all $u \in \mathcal{T}$, $Q(u) \geq Q(u^*)$. In addition, there exists an admissible initialization set $\mathcal{V}$, which is a nonempty, *known* compact subset of $\mathcal{T}$.

Remark 4. First, Assumption 3 states that there exist some system input that solves the constrained optimization problem in (5). This assumption requires that the optimization problem is well-defined. Second, Assumption 3 states that we have some limited knowledge about the admissible set $\mathcal{T}$, namely, the known admissible initialization set $\mathcal{V}$, such that we can initialize well within this admissible set. This is a reasonable assumption in practice since we usually have some knowledge about where we can initialize our system without violating the constraints immediately. For example, this assumption is satisfied in our industrial case study in Section 5.

In this work, we will solve the steady-state constrained optimization problem in (5) by finding a near-optimal system input u^* for the class of dynamical systems as in Definition 1, which satisfies Assumptions 2 and 3, i.e., we will solve the problem by finding a near-optimal system input for which constraint satisfaction ($G(u) \leq 0$) is achieved in steady-state, and which can only be assessed on the basis of measurable constraint functions. Thereto, in the next section we will present a class of algorithms that exploits barrier function methods and that provides an arbitrarily close solution to the constrained optimization problem in (5), based on output measurements y and z, and generated by the system in Definition 1.

Remark 5. Examples of often studied dynamical systems in the extremum-seeking literature are, for example, dynamical systems with steady-state equilibria, see, e.g., Krstić and Wang (2000), Tan, Nešić, and Mareels (2006), and dynamical systems with periodically time-varying steady-state responses, see, e.g., Haring, van de Wouw, and Nešić (2013). The presented class of systems covers these examples in the presence of multiple measurable outputs, in which one output is related to a to-be-optimized measurable cost and all other outputs are related to measurable constraint functions.

3. Class of optimization algorithms for constrained optimization problems using barrier function methods

In this section, firstly, we discuss classical barrier function methods to address constrained optimization problems of the form in (5), see, e.g., Fiacco and McCormick (1990). Secondly, in the spirit of the class of algorithms for unconstrained optimization problems presented in Teel (2000a), we introduce a mathematical description of a class of algorithms that enables constrained optimization by means of barrier function methods.

3.1. Constrained optimization using barrier function methods

The barrier function method is a well-known approach to address constrained optimization problems. Namely, it allows to approximate constrained optimization problems of the form in (5) by an unconstrained *modified* optimization problem. The approximation of the actual constrained optimization problem can be attributed to the nature of the barrier function method. In particular, barrier functions establish a barrier on the boundary of the admissible set $\mathcal{T}$, thereby preventing any optimization algorithm that starts well within the admissible set to reach the boundary of the admissible set. We adopt the following definition.

Definition 6. Let $\mathcal{T}$ be the admissible set as defined in Assumption 3. Let $\mathcal{T}^o$ and $\partial\mathcal{T}$ denote the interior and the boundary of the admissible set $\mathcal{T}$, respectively. For each $\mu \in \mathbb{R}_{>0}$, called the barrier parameter, a barrier function $B : \mathcal{T}^o \times \mathbb{R}_{>0} \to \mathbb{R}$, is defined on $\mathcal{T}^o$ such that

- $B(u, \mu)$ is continuous for $u \in \mathcal{T}^o$ and $\mu \in \mathbb{R}_{>0}$,
- $B(u, \mu) \to 0$ for $u \in \mathcal{T}^o$ and $\mu \to 0$,
- $B(u, \mu) \to \infty$ for $\|u\|_{\partial\mathcal{T}} \to 0$ and $\mu \in \mathbb{R}_{>0}$.

Barrier functions that satisfy Definition 6 are, for example, the so-called logarithmic and inverse barrier functions, see, e.g., Fiacco and McCormick (1990).

By exploiting barrier functions as defined in Definition 6, we can approximate the constrained optimization problem in (5) by the following unconstrained modified optimization problem:

$$\min_{u \in \mathcal{T}^o} \tilde{Q}(u, \mu), \tag{6}$$

with $\tilde{Q}(u, \mu) := Q(u) + B(u, \mu)$ the so-called modified objective function. We call the solution to (6) an *approximate minimizer*, where $\tilde{\mathcal{C}}_{\mathcal{T}}$ denotes the set of approximate minimizers, i.e., for any $\mu \in \mathbb{R}_{>0}$ there exist system inputs $u^* \in \tilde{\mathcal{C}}_{\mathcal{T}} \subset \mathcal{T}^o$ such that for all $u \in \mathcal{T}^o$, $\tilde{Q}(u, \mu) \geq \tilde{Q}(u^*, \mu)$. The fact that, for constrained optimization problems, a barrier function method only provides approximate solutions is particularly evident in cases where solutions to the actual constrained optimization problem in (5) are located on the boundary of the admissible set $\partial\mathcal{T}$, i.e., when the intersection of the boundary of the admissible set and the set of exact minimizers is nonempty, i.e., $\partial\mathcal{T} \cap \mathcal{C}_{\mathcal{T}}$ is nonempty. Namely, in cases where optimization algorithms employ barrier functions, we have that the boundary of the admissible set and the set of approximate minimizers do not intersect, i.e., $\partial\mathcal{T} \cap \tilde{\mathcal{C}}_{\mathcal{T}} = \emptyset$. Nevertheless, we would like to stress that, in practice, the set of approximate minimizers $\tilde{\mathcal{C}}_{\mathcal{T}}$ can be made arbitrarily close to the actual set of minimizers $\mathcal{C}_{\mathcal{T}}$ by having a sufficiently small barrier parameter μ. Namely, for a sufficiently small $\mu \in \mathbb{R}_{>0}$ and $u \in \mathcal{T}^o$, from Definition 6 it follows that $B(u, \mu) \approx 0$, and thus $\tilde{Q}(u, \mu) \approx Q(u)$. Next, we will mathematically describe the class of algorithms that enables constrained optimization by means of barrier function methods.

3.2. Characterization of constrained optimization algorithms

In this section, we introduce a class of algorithms, inspired by barrier function methods, and designed to induce convergence to the set of approximate minimizers $\tilde{\mathcal{C}}_{\mathcal{T}}$. The class of algorithms that is described here is based on *exact* evaluation of the steady-state input–output mappings Q and G in (3), that is, the outputs y and z are not affected by system dynamics, leading to exact evaluation of the steady-state system performance Q and steady-state constraint functions G, respectively. Moreover, we consider the evaluation of Q and G for a particular input u to be readily available. Later in Section 4, we will show how to exploit the introduced class of algorithms in an extremum-seeking control context, in which (1) the evaluation of the steady-state input–output mappings Q and G is obtained sequentially, and (2) the output measurements are affected by (transient) dynamical behavior of the system. Therein, we consider the steady-state system performance Q and steady-state constraint functions G to be available approximately only through measurable outputs y and z.

Let us consider optimization algorithms described by the following difference inclusion (see also, e.g., Teel and Popović (2001)):

$$\Sigma : \qquad u^+ \in F(u, Y(u), Z(u)), \tag{7}$$

where $F : \mathbb{R}^{n_u} \times \mathbb{R}^{n_v} \times \mathbb{R}^{n_v \times n_z} \to \mathbb{R}^{n_u}$ is a set-valued map for which the update u^+ can be any element of the set, the function $Y \in \mathbb{R}^{n_v}$ contains all information regarding (the gradient of) the cost near u, and the function $Z \in \mathbb{R}^{n_v \times n_z}$ carries all information about (the gradient of) the constraint functions near u. In particular, Y and Z are respectively defined as follows:

$$Y(u) := \begin{bmatrix} Q(u + v_1(u)) \\ \vdots \\ Q(u + v_{n_v}(u)) \end{bmatrix}, \tag{8}$$

$$Z(u) := \begin{bmatrix} G_1(u+v_1(u)) & \dots & G_{n_z}(u+v_1(u)) \\ \vdots & \ddots & \vdots \\ G_1(u+v_{n_v}(u)) & \dots & G_{n_z}(u+v_{n_v}(u)) \end{bmatrix}, \tag{9}$$

where $v_j(\cdot) \in \mathbb{R}^{n_u}$, with $j = 1, \dots, n_v$, are user-defined dither functions that may depend on u, $Q(\cdot)$ and $G(\cdot)$ are the steady-state input–output maps as defined Assumption 2, and G_i denotes the ith element of G, that is, the ith steady-state constrained output. The user-defined dither signal may depend on the chosen optimization algorithm used for the particular optimization problem at hand, and its numerical implementation. We will adopt the following assumption on optimization algorithms as in (7)–(9), which can be seen as a generalization of the assumptions on the class of algorithms used in Teel and Popović (2001).

Assumption 7. Let $\mathcal{T}$ be the admissible set as defined in Assumption 3, with $\mathcal{T}^o$ and $\partial\mathcal{T}$ the interior and the boundary of the admissible set $\mathcal{T}$, respectively. Let $\tilde{\mathcal{C}}_{\mathcal{T}}$ be the set of approximate constrained minimizers. Let us adopt the following assumption:

- For each input $u \in \mathcal{T}^o$, the set $F(u, Y(u), Z(u))$ in (7) is nonempty and compact. Moreover, the set F is an upper semi-continuous function of u.
- We assume that there exist a locally Lipschitz function $V_\Sigma : \mathbb{R}^{n_u} \to \mathbb{R}_{\geq 0}$, which is radially unbounded on the admissible set $\mathcal{T}$, a nonnegative constant $\delta \in \mathbb{R}_{\geq 0}$, and $\mathcal{K}_\infty$-functions $\alpha(\cdot)$ and $\rho(\cdot)$, such that

$$\begin{aligned} V_\Sigma(u) &= 0 && \forall\, u \in \tilde{\mathcal{C}}_{\mathcal{T}}, \\ \alpha(\|u\|_{\tilde{\mathcal{C}}_{\mathcal{T}}}) \leq V_\Sigma(u) & && \forall\, u \in \mathcal{T}^o, \\ V_\Sigma(u) &\to \infty && \text{for } \|u\|_{\partial\mathcal{T}} \to 0, \\ \max_{w \in F(u,Y(u),Z(u))} V_\Sigma(w) - V_\Sigma(u) &\leq \\ -\rho(V_\Sigma(u)) + \delta & && \forall\, u \in \mathcal{T}^o. \end{aligned} \tag{10}$$

- We assume that the constant $\delta \in \mathbb{R}_{\geq 0}$ can be made arbitrarily small by tuning the parameters of the optimization algorithm F in (7).

Remark 8. The existence of a function V_Σ satisfying the associated conditions stated in Assumption 7 are motivated by converse Lyapunov theorems for stability of discrete-time systems on arbitrary sets, see, e.g., Kellett (2015), Kellett and Teel (2004) and Teel and Praly (2000). Moreover, radial unboundedness of V_Σ on the admissible set $\mathcal{T}$ is motivated by the use of barrier functions in the constrained optimization problem. Also note that the first and third condition in (10) imply that the set of approximate minimizers $\tilde{\mathcal{C}}_{\mathcal{T}}$ and the boundary of the admissible set $\partial\mathcal{T}$ do not intersect.

Remark 9. In Assumption 7, the size of the nonnegative constant δ in (10) can typically be influenced by tunable parameters of the optimization algorithm F described by the class of algorithms in (7)–(9). To motivate this further, consider, for example, the minimization of a convex and differentiable function $\tilde{Q}(u)$ on $\mathcal{T}^o$, with $\tilde{Q}(u) \to \infty$ for $\|u\|_{\partial\mathcal{T}} \to 0$. Moreover, for any $u \in \bar{\mathcal{T}}$, with $\bar{\mathcal{T}}$ a strict subset of $\mathcal{T}^o$, suppose there exists an $M > 0$ such that $\|\nabla^2 \tilde{Q}(u)\| \leq M$ for all $u \in \bar{\mathcal{T}}$. Let us employ, a gradient descent optimization algorithm F for which the gradient is estimated based on a central difference scheme with dither function $v(u) := c_v \in \mathbb{R}_{>0}$ and exact evaluation of the function $\tilde{Q}$ as follows:

$$F(u, Y(u), Z(u)) := u - \lambda \left(\frac{\tilde{Q}(u + c_v) - \tilde{Q}(u - c_v)}{2c_v} \right), \tag{11}$$

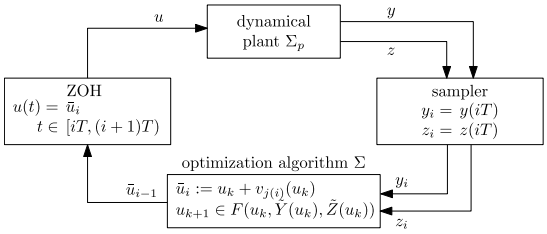

Fig. 1. Sampled-data extremum-seeking control framework with multiple output channels.

with $\lambda \in \mathbb{R}_{>0}$. Let us take function $V_\Sigma(u) := \tilde{Q}(u) - \tilde{Q}(u^*)$, with u^* the extremum for which it holds that $\nabla\tilde{Q}(u^*) = 0$. This $V_\Sigma(u)$ satisfies the conditions in (10). With this $V_\Sigma(u)$, we obtain that $V_\Sigma(u^+) - V_\Sigma(u) \leq -\lambda(\nabla V_\Sigma(u))^2 + \delta$, with $\delta := M^3\lambda^2 c_v^2$, $\lambda \in (0, \frac{1}{M})$. The constant δ can be made arbitrarily small by selecting sufficiently small λ and c_v.

In the next section, we will analyze the dynamic behavior of the interconnection of a dynamical system described in Definition 1, and an optimization algorithm of the form in (7)–(9) in an online extremum-seeking control implementation.

4. Stability of the interconnected class of dynamical systems and a class of extremum seeking algorithms

In this section, we aim to investigate the dynamic behavior of a discrete-time system that describes the closed-loop feedback interconnection of the class of dynamical systems from Section 2, denoted by Σ_p, and the class of algorithms discussed in Section 3, denoted by Σ, in an extremum-seeking context. In particular, we consider the interconnection of a dynamical system Σ_p and an optimization algorithm Σ through a T-periodic sampler, and a zero-order-hold (ZOH) element, see Fig. 1. We analyze the dynamic behavior of the closed-loop feedback interconnection in the case where the elements of the functions Y and Z in (8) and (9), respectively, (1) can only be obtained sequentially by performing n_v experiments and evaluating the steady-state input–output mappings Q and G after each experiment, and (2) can only be based on (periodically) sampling the outputs y and z, providing mere approximations of the steady-state input–output mappings Q and G, respectively.

Next, we describe the extremum-seeking algorithm performing n_v experiments to realize one update of the system input u, based on a so-called waiting time T that prescribes the duration of each experiment, and on approximations of the steady-state input–output mappings Q and G obtained via the collection of the corresponding output measurements each T seconds.

Algorithm 1. Consider the interconnection of the dynamical system Σ_p and an optimization algorithm Σ through a T-periodic sampler, and a zero-order-hold (ZOH) element as in Fig. 1. Suppose that the waiting time T, the number of experiments n_v to realize one iteration of the optimization algorithm, and the initial algorithm state u_0 are specified. Let us define the ideal periodic sampling operation $x_i := x(iT)$:

$$\begin{aligned} y_i &:= y(iT) \quad \forall\, i = 0, 1, \dots, \\ z_i &:= z(iT) \quad \forall\, i = 0, 1, \dots, \end{aligned} \tag{12}$$

where y_i and z_i are the collected measurements as used by the optimization algorithm, where $i \in \mathbb{N}$ denotes the T-periodic sampling index. Define the ZOH operation as follows:

$$u(t) := \bar{u}_i \quad \forall\, t \in [iT, (i+1)T), \tag{13}$$

with sampling index $i = 0, 1, \ldots$, waiting time $T > 0$, and step input parameter $\bar{u}_i$. For sampling index i, the step input parameter $\bar{u}_i$ is determined by the state of the optimization algorithm u_k as follows:

$$\bar{u}_i := u_k + v_{j(i)}(u_k) \quad \forall\, i = 0, 1, \ldots, \tag{14}$$

with $k \in \mathbb{N}$ the optimization algorithm index, u_0 the initial algorithm state, and dither functions $v_{j(i)}$ with dither index $j \in \{1, \ldots, n_v\}$. The dither index j is related to the T-periodic sampling index i and the number of experiments n_v required to realize one iteration of the optimization algorithm through $j(i) := (i \bmod n_v) + 1$. The optimization algorithm index k is related to the T-periodic sampling index i and the number of experiments n_v through $k = \left\lfloor \frac{i}{n_v} \right\rfloor$. The optimization algorithm is characterized by the mapping F given in (7), which exploits the collected measurements y_i and z_i:

$$u_{k+1} \in F(u_k, \tilde{Y}(u_k), \tilde{Z}(u_k)) \quad \forall\, k = 0, 1, \ldots, \tag{15}$$

with functions $\tilde{Y}(u_k)$ and $\tilde{Z}(u_k)$ defined as follows:

$$\tilde{Y}(u_k) := \begin{bmatrix} y_{kn_v+1} \\ \vdots \\ y_{(k+1)n_v} \end{bmatrix}, \quad \tilde{Z}(u_k) := \begin{bmatrix} z_{kn_v+1}^\top \\ \vdots \\ z_{(k+1)n_v}^\top \end{bmatrix}, \tag{16}$$

which, following from the definitions of the output channels $y(t)$ and $z(t)$ in (2), are approximations of the functions $Y(u_k)$ and $Z(u_k)$ in (8) and (9), respectively, for sufficiently long waiting time T.

Example 10. To illustrate the sequence of inputs generated by Algorithm 1 and the corresponding measured outputs of the system Σ_p, consider the table below which provides an example of the sequence of inputs and outputs at different sampling indexes i, with the initial algorithm state u_0, and the number of experiments $n_v = 3$ to perform one update of the state of the optimization algorithm and generated by Algorithm 1.

i	y_i, z_i	input $\bar{u}_i$	u_k, $k := \left\lfloor \frac{i}{n_v} \right\rfloor$
0	–	$\bar{u}_0 = u_0 + v_1(u_0)$	u_0 is user-defined
1	y_1, z_1	$\bar{u}_1 = u_0 + v_2(u_0)$	–
2	y_2, z_2	$\bar{u}_2 = u_0 + v_3(u_0)$	–
3	y_3, z_3	$\bar{u}_3 = u_1 + v_1(u_1)$	$u_1 \in F(u_0, \tilde{Y}, \tilde{Z})$

The first column represents the sampling index i. The second column represents the sampled output measurements y_i and z_i at $t = iT$. The third column represents the step input parameter $\bar{u}_i$, applied to the system Σ_p through the ZOH element $u(t) = \bar{u}_i$ for $t \in [iT, (i+1)T)$. The step input parameter $\bar{u}_i$ is determined by the algorithm state u_k, with $k = \left\lfloor \frac{i}{n_v} \right\rfloor$ and the dither function $v_{j(i)}(u_k)$, with $j(i) := (i \mod n_v) + 1$. The algorithm state u_k in the fourth column is generated by the optimization algorithm described by (15) on the basis of the functions $\tilde{Y}(u_k)$ and $\tilde{Z}(u_k)$ defined in (16).

For example, at sampling index $i = 1$, we have collected the output measurements y_1 and z_1 at $t = T$, which are generated by applying the step input $u(t) = \bar{u}_0$ during $t \in [0, T)$ to the system. A new step input $u(t) = \bar{u}_1$ is determined and applied during $t \in [T, 2T)$. At sampling index $i = 2$, we sample the outputs y_2 and z_2. A new step input $u(t) = \bar{u}_2$ is determined and applied during $t \in [2T, 3T)$. At sampling index $i = 3$, we sample the outputs y_3 and z_3. After performing $n_v = 3$ experiments and sampling the output measurements after each experiment, the algorithm state u_0 is updated to $u_1 \in F(u_0, \tilde{Y}, \tilde{Z})$.

To account for the discrepancy between the steady-state input–output mappings $Q(u)$ and $G(u)$ and the actual measurements y and z, we need the following additional assumption, partially adopted from Teel and Popović (2001).

Assumption 11. For the plant Σ_p described in Definition 1, it holds that

- for each $\Delta_{\mathcal{U}}, \Delta_{\mathcal{X}} \in \mathbb{R}_{>0}$, there exist $L_H, L_G \in \mathbb{R}_{>0}$ such that, for any input $u \in \mathcal{T}$ with $\|u\|_{\tilde{\mathcal{C}}_{\mathcal{T}}} \leq \Delta_{\mathcal{U}}$, and any $\|x\|_{\mathcal{A}(u)} \leq \Delta_{\mathcal{X}}$, we have the following inequalities:
$$\begin{aligned} &\|h(x) - Q(u)\| \leq L_H \|x\|_{\mathcal{A}(u)}, \\ &\|g(x) - G(u)\| \leq L_G \|x\|_{\mathcal{A}(u)}. \end{aligned} \tag{17}$$
- the set-valued map $\mathcal{A}(\cdot)$ is locally Lipschitz; in particular, for each $\Delta_{\mathcal{U}} > 0$, there exists an $L_{\mathcal{A}} > 0$ such that
$$\begin{aligned} &\max\{\|u_1\|_{\tilde{\mathcal{C}}_{\mathcal{T}}}, \|u_2\|_{\tilde{\mathcal{C}}_{\mathcal{T}}}\} \leq \Delta_{\mathcal{U}} \Rightarrow \\ &\mathcal{A}(u_1) \subseteq \mathcal{A}(u_2) + L_{\mathcal{A}} \|u_1 - u_2\| \bar{\mathcal{B}}, \\ &\text{with } u_1, u_2 \in \mathcal{T}. \end{aligned} \tag{18}$$

For the optimization algorithm F as described in (7) which satisfies the properties stated in Assumption 7, the following assumptions hold:

- Take any $u_{\tilde{F}}$ generated by $F(u, \tilde{Y}(u), \tilde{Z}(u))$, and let u_F be its closest point in the set $F(u, Y(u), Z(u))$. Then, for each $\Delta_{\mathcal{U}}, \Delta \in \mathbb{R}_{>0}$, there exist $L_Y, L_Z \in \mathbb{R}_{>0}$ such that for any input $u \in \mathcal{T}^o$ with $\|u\|_{\tilde{\mathcal{C}}_{\mathcal{T}}} \leq \Delta_{\mathcal{U}}$, and $\|\tilde{Y}\|, \|\tilde{Z}\| \leq \Delta$, we have
$$\|u_{\tilde{F}} - u_F\| \leq L_Y \|\tilde{Y}(u) - Y(u)\| + L_Z \|\tilde{Z}(u) - Z(u)\|. \tag{19}$$
- For the perturbation functions $v_j(\cdot)$ we assume that, for each $\Delta_{\mathcal{U}} \in \mathbb{R}_{>0}$ and for any $u \in \bar{\mathcal{T}}$, with $\bar{\mathcal{T}}$ an arbitrary (large) strict subset of $\mathcal{T}^o$ and $\|u\|_{\tilde{\mathcal{C}}_{\mathcal{T}}} \leq \Delta_{\mathcal{U}}$, there exist (sufficiently small) constants $M_v, c_v \in \mathbb{R}_{\geq 0}$ such that, for each $j = 1, \ldots, n_v$, we have that
$$\|v_j(u)\| \leq M_v \|u\|_{\tilde{\mathcal{C}}_{\mathcal{T}}} + c_v. \tag{20}$$

The next lemma states the outcome of the interconnected discrete-time system after one update of the optimization algorithm, i.e., one sequence of inputs generated by Algorithm 1. In particular, define a state $\bar{x}_k := x_{kn_v}$ denoting the state of Σ_p at the beginning of the $(k+1)$th sequence of inputs, where k denotes the optimization algorithm index. The outcome of one sequence of inputs as considered in Lemma 12 is an important stepping stone in the proof of Theorem 13 to show (1) convergence of the algorithm state u_k to a neighborhood of the set of approximate minimizers $\tilde{\mathcal{C}}_{\mathcal{T}}$ and (2) steady-state constraint satisfaction for all system inputs, over multiple input sequences.

Lemma 12. *Suppose that the system Σ_p and the algorithm Σ satisfy Assumptions 2, 3, 7 and 11. Let the system Σ_p and algorithm Σ be connected as described in Algorithm 1. Then, for any $\epsilon_1 \in (0, 1]$, any $\epsilon_2, \Delta_{\mathcal{X}}, \Delta_{\mathcal{U}} \in \mathbb{R}_{>0}$, and an arbitrary (large) strict subset $\bar{\mathcal{T}} \subset \mathcal{T}^o$, there exists a waiting time $T^* \geq T$, with T as in Assumption 2, such that, for any $\bar{x} \in \mathcal{X}$ with $\|\bar{x}\|_{\mathcal{A}(u+v_{n_v}(u))} \leq \Delta_{\mathcal{X}}$, and any $u \in \bar{\mathcal{T}}$ with $\|u\|_{\tilde{\mathcal{C}}_{\mathcal{T}}} \leq \Delta_{\mathcal{U}}$, respectively being the states of the plant and the algorithm at the beginning of the current input sequence, the states of the system and algorithm at the beginning of the next input sequence are given as follows:*

$$\begin{aligned} &u^+ \in F(u, \tilde{Y}(u), \tilde{Z}(u)), \ \ \psi^+ = u, \\ &\bar{x}^+ \in \mathcal{A}(u + v_{n_v}(u)) + \Bigg(\epsilon_1 \Bigg(\|\bar{x}\|_{\mathcal{A}(u+v_{n_v}(u))} \\ &\qquad + L_{\mathcal{A}} \sum_{j=1}^{n_v} \|v_j(u) - v_{j-1}(u)\| \Bigg) + n_v \epsilon_2 \Bigg) \bar{\mathcal{B}}, \end{aligned} \tag{21}$$

where ψ is a memory state, $\tilde{Y}(u)$ and $\tilde{Z}(u)$ are given in (16), and $v_0(u) := v_{n_v}(u)$.

Proof. The proof of Lemma 12 can be found in Appendix A. □

For the purpose of the stability analysis let us now define the following function

$$W(\psi, \bar{x}, u) := V_{\Sigma_p}(\psi, \bar{x}) + 2V_{\Sigma}(u), \tag{22}$$

where $V_{\Sigma_p}(\psi, \bar{x}) := \sigma \|\psi\|_{\tilde{\mathcal{C}}_{\mathcal{T}}} + \|\bar{x}\|_{\mathcal{A}(\psi + v_{n_v}(\psi))}$ with some constant $\sigma \in \mathbb{R}_{>0}$. Let us define the following increments:

$$\begin{aligned} \Delta W(\psi, \bar{x}, u) &:= W(\psi^+, \bar{x}^+, u^+) - W(\psi, \bar{x}, u), \\ \Delta V_{\Sigma_p}(\psi, \bar{x}) &:= V_{\Sigma_p}(\psi^+, \bar{x}^+) - V_{\Sigma_p}(\psi, \bar{x}), \\ \Delta V_{\Sigma}(u) &:= V_{\Sigma}(u^+) - V_{\Sigma}(u). \end{aligned} \tag{23}$$

The next result states conditions on the initial conditions and parameters of the ESC algorithm (such as the waiting time), such that the system input u converges to an arbitrarily small neighborhood of the set of approximate minimizers $\tilde{\mathcal{C}}_{\mathcal{T}}$, while steady-state constraint satisfaction is guaranteed all along the evolution of the optimization iterations.

Theorem 13. *Suppose that the system Σ_p and the algorithm Σ satisfy Assumptions 2, 3, 7 and 11. Let the system Σ_p and algorithm Σ be interconnected as described in Algorithm 1. For any $u_0, \psi_0 \in \mathcal{V} \subset \bar{\mathcal{T}}$ with $\bar{\mathcal{T}}$ an arbitrary (large) strict subset of $\mathcal{T}^o$ and $\bar{x}_0 \in \mathcal{X}$, with $\|u_0\|_{\tilde{\mathcal{C}}_{\mathcal{T}}} \leq \Delta_{\mathcal{U}}$, $\|\psi_0\|_{\tilde{\mathcal{C}}_{\mathcal{T}}} \leq \Delta_{\mathcal{U}}$, and $\|\bar{x}_0\|_{\mathcal{A}(\psi + v_{n_v}(\psi_0))} \leq \Delta_{\mathcal{X}}$ with some $\Delta_{\mathcal{U}}, \Delta_{\mathcal{X}} \in \mathbb{R}_{>0}$, there exists a sufficiently large waiting time $T^* \geq T$, with T as in Assumption 2, and $\mathcal{K}_\infty$-function $\tilde{\gamma}(\cdot)$ such that we obtain the following increment:*

$$\Delta W(\psi, \bar{x}, u) \leq -\tilde{\gamma}(W(\psi, \bar{x}, u)) + 2\delta + \gamma + \delta_V, \tag{24}$$

for arbitrarily small $\delta, \gamma \in \mathbb{R}_{>0}$, and any small $\delta_V \in \mathbb{R}_{>0}$. Moreover, there exist $\Delta_W \in \mathbb{R}_{\geq 0}$, $\mathcal{K}_\infty$-function $\hat{\rho}(\cdot)$, and $\mathcal{KL}$-function $\hat{\beta}(\cdot, \cdot)$, such that

$$\begin{aligned} W(\psi_k, \bar{x}_k, u_k) \leq \max\{&\hat{\beta}(W(\psi_0, \bar{x}_0, u_0), k), \\ &\tilde{\gamma}^{-1} \circ \hat{\rho}^{-1}(2\delta + \gamma + \delta_V)\}, \end{aligned} \tag{25}$$

holds for all $k \in \mathbb{N}$, with $W(\psi_0, \bar{x}_0, u_0) \leq \Delta_W$.

As a consequence:

- *$V_\Sigma(u_k)$ is bounded for all $k \in \mathbb{N}$, which implies that $u_k \in \mathcal{T}^o$ for all $k \in \mathbb{N}$, i.e., steady-state constraint satisfaction is guaranteed and*
- *the solutions of the closed-loop system converge to a set $\mathcal{Y}_u := \{u \in \mathcal{T}^o \mid \|u\|_{\tilde{\mathcal{C}}_{\mathcal{T}}} \leq \frac{1}{2}\alpha^{-1}\big(\frac{1}{2}\tilde{\gamma}^{-1} \circ \hat{\rho}^{-1}(2\delta + \gamma + \delta_V)\big)\}$, with $\alpha \in \mathcal{K}_\infty$ defined in Assumption 7, where this set can be made arbitrarily small.*

Proof. The proof of Theorem 13 can be found in Appendix B. □

Remark 14. We would like to emphasize that a local result, i.e., within a subset of the admissible set $\mathcal{T}$, can easily be derived by using a similar approach, but is omitted for space reasons.

Remark 15. The set $\mathcal{Y}_u$ to which the solutions of the closed-loop system converge can be made arbitrarily small. Namely, (1) $\delta_V \in \mathbb{R}_{>0}$ can be any arbitrarily small constant, (2) we can make γ arbitrarily small by choosing a sufficiently large waiting time $T \in \mathbb{R}_{>0}$, and (3) δ, which is defined in Assumption 7, can typically be tuned sufficiently small by tuning the parameters of the optimization algorithm F (see also Assumption 7 and Remark 9). However, we would like to emphasize that making γ and δ small can lead to a slower convergence in practice. Namely, a longer waiting time T (i.e., a smaller γ) implies that each evaluation of the system's objective function requires more time while the optimization algorithm requires multiple evaluations. Moreover, having a smaller δ by appropriately tuning the parameters of the optimization algorithm typically leads to an increased number of input updates that are needed to reach the set $\mathcal{Y}_u$ and therefore can also lead to a slower convergence.

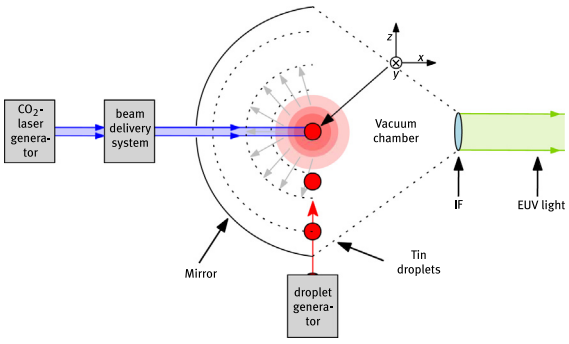

Fig. 2. Schematic representation of an LPP source system, with the laser-to-droplet (L2D) relative coordinate frame.

Remark 16. Inequality (25) also expresses a decaying bound on the transient solutions of the closed-loop system. Since W expresses both the distance of the plant response to the steady state and the distance of the input u to the minimizer in a combined fashion we do not provide a transient bound on these effects individually.

Remark 17. The result presented in Theorem 13 is focused on achieving the optimal input that satisfies the output constraints in steady-state. We emphasize that, under the conditions of Theorem 13, constraint satisfaction is also guaranteed during the transients of the extremum seeker if the plant output would be on its steady-state response. Constraint satisfaction on the output responses during the transient of the plant itself is, however, not guaranteed. To accomplish this, additional assumptions on the class of plants would be required. In particular, system properties would need to be defined on compact subsets, and additional assumptions on initial data and on the transient behavior of the plant are required. This extended problem setting is not considered in this work.

5. Industrial case study: constrained optimization of EUV light generation in a Laser Produced Plasma (LPP) source

The semiconductor industry continues to develop lithographic technologies which are able to realize ever-smaller integrated circuit dimensions. Extreme ultraviolet lithography, a next-generation lithography technology, is able to produce sub-nanometer features by exposing substrates, such as silicon wafers, to extreme ultraviolet (EUV) light. The necessary EUV light is typically produced by a so-called Laser Produced Plasma (LPP) source, which is the most promising approach for providing power output that is scalable to meet the needs of high volume production exposure tools. However, achieving and maintaining optimal EUV light generation is a challenging task. In this section, we provide a description of a typical LPP source and discuss the constrained optimization problem associated to its performance. Moreover, we present a representative LPP source model, and employ the constrained sampled-data extremum-seeking approach proposed in this paper to achieve optimal EUV light generation.

5.1. System description

LPP sources produce EUV light by converting a material that has emission lines in the EUV spectrum, e.g., lithium or tin, into a plasma state that ultimately emits the desired EUV photons. Fig. 2 schematically depicts a typical LPP source system and its most crucial components: (1) a CO_2 laser generator, (2) a laser beam delivery system, (3) a vacuum chamber, (4) a droplet generator,

(5) a spherical mirror, the so-called collector, and (6) an intermediate focus (IF). Inside the vacuum chamber, the EUV-emitting plasma is generated by irradiating droplets of material with a high-energy pulsating CO_2 laser beam. The droplet generator fires small droplets at a rate of 50 kHz into the vacuum chamber. The beam delivery system orients and focusses the high-energy pulsating CO_2 laser beam in such a way that it hits the traveling droplets inside the vacuum chamber. If the droplets are hit correctly, EUV photons are generated by the irradiated material, reflected by the collector, and transmitted towards the IF. Here, the transmitted EUV photons enter the EUV lithography scanner and enable the patterning of sub-nanometer features on a silicon wafer.

To cope with the various losses of EUV intensity within the lithography scanner, and still enable patterning of sub-nanometer features on a silicon wafer using the lithography scanner, the EUV light generated by the light source needs to be maximized. The intensity of the generated EUV light highly depends on the position of the laser beam with respect to the droplet. Due to the complex (plasma) physics involved, the complex interactions between the droplets, laser and plasma, and the difficulty of accurately measuring the position of the laser beam relative to the droplet (amongst other challenges), models of the LPP system based on first-principles tend to be inaccurate in describing the actual system behavior. As such, employing the optimal laser position obtained from such a first principle model on the actual system is likely to yield sub-optimal EUV intensity. Instead, data-based methods such as ESC can be employed to adjust the laser position in y- and z-direction (see Fig. 2) in real-time to optimize the EUV intensity, based on real-time measurements of the EUV intensity.

Optimizing average EUV light generation using classical (continuous-time, unconstrained) ESC was proposed in Frihauf, Riggs, Graham, Chang, and Dunstan (2013). That approach, however, does not take into account any (unknown) disturbances, which can lead to undesirably high peak-to-peak variations in the generated EUV intensity for certain laser orientations. In addition, laser light that is being reflected back to the CO_2 laser generator itself, referred to as the back-reflection and which is continuously being monitored, can damage the LPP source if it exceeds some threshold value. Therefore, we employ the developed constrained sampled-data extremum-seeking control strategy to maximize the average EUV intensity while avoiding (1) large variations of EUV intensity, and (2) excessive back-reflection.

5.2. LPP source model

The LPP system under study is modeled[1] by an asymptotically stable linear-time-invariant (LTI) dynamical system subject to external period disturbances, representing a closed-loop mirror control system (modeling the beam delivery system in Fig. 2), followed by an experimentally obtained static nonlinear model for the effect of the laser positioning on the EUV intensity and the laser back reflection (capturing the complex plasma physics of the source). Note that the LPP system model under study satisfies Assumptions 2 and 11 since the system is LTI and asymptotically stable. We emphasize that especially the static nonlinear model, describing the effect of the laser positioning on the EUV intensity and the laser back reflection, is typically hard (and time-consuming) to obtain in practice, which motivates the use of a data-based approach such as ESC for performance optimization. Here, we employ such experimentally obtained model in support of the simulation study. Finally, and user-defined filters are included to obtain as measured outputs the average EUV intensity, the peak-to-peak EUV intensity, and the laser back reflection signal to be used as input for the extremum-seeking controller see Fig. 3 for a schematic overview of the model.

[1] To protect the company's interests, a more detailed description of the LPP model than the one presented here, and units of certain variables, are omitted. Moreover, values of variables are normalized or scaled.

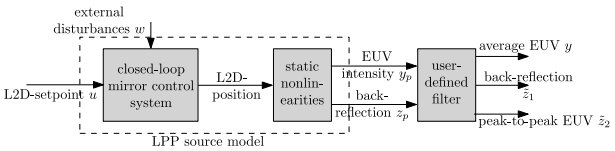

Fig. 3. Model of the LPP source.

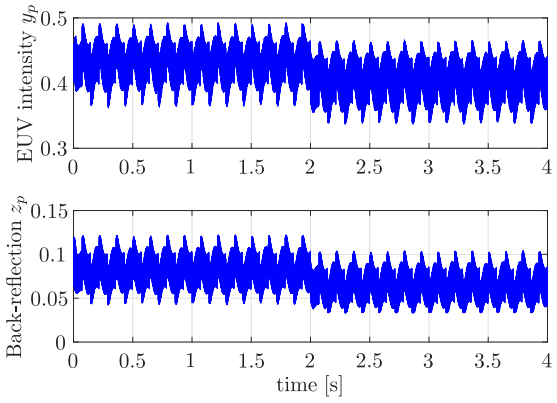

Fig. 4. The EUV intensity (top) and the back-reflection signal (bottom) as a function of time for two L2D-setpoints; (1) $\text{L2D}_y = -0.225$ [normalized] and $\text{L2D}_z = 0.4$ [normalized] during $t \in [0, 2]$ s, and (2) $\text{L2D}_y = -0.275$ [normalized] and $\text{L2D}_z = 0.4$ [normalized] during $t \in (2, 4]$ s.

5.2.1. Closed-loop mirror control system

The closed-loop mirror control system basically comprises the laser orientation part of the beam delivery system of the LPP source. The laser orientation part of the beam delivery system consists of (a set of) adjustable mirrors, able to adjust the laser-to-droplet (L2D) positioning in the y- and z-direction on the basis of a stable feedback control design. The feedback controller uses the L2D-positions, measured indirectly using data obtained through various sensors, and user-defined L2D-setpoints to minimize the L2D-setpoint errors. The closed-loop mirror control system model takes into account disturbances such as laser–droplet interactions, various (high- and low-frequency) disturbances ranging from $1 \cdot 10^{-3} - 300$ Hz, and white noise, that affect the L2D-position measurements. The disturbances are modeled as T_w-periodic external disturbances w which are supplied to the closed-loop mirror control system, with $T_w = 2$ s.

5.2.2. Static nonlinearities

The static nonlinearities in the LPP source model provide mappings from the L2D-position to (1) the EUV intensity, denoted by y_p, and (2) the back-reflection, denoted by z_p. These output nonlinearities are experimentally obtained from an industrial LPP source system for the purpose of modeling. Fig. 4 depicts the EUV intensity y_p and the back-reflection signal z_p as a function of time for two particular L2D-setpoints, obtained using the simulation model. Due to the T_w-periodic nature of the external disturbances, the measured outputs are T_w-periodic as well.

5.2.3. User-defined filtering

On the basis of the measurable EUV intensity y_p and back-reflection z_p, and the T_w-periodic nature of these outputs, the

following filters are defined that determine the average EUV intensity y, the maximum back-reflection signal $\tilde{z}_1$, and the peak-to-peak EUV variation $\tilde{z}_2$ as follows:

$$\begin{aligned} y(t) &:= \frac{1}{T_w}\int_{t-T_w}^{t} y_p(\tau)d\tau,\ \tilde{z}_1(t) := \max_{\tau\in[t-T_w,t)} z_p(\tau), \\ \tilde{z}_2(t) &:= \max_{\tau\in[t-T_w,t)} y_p(\tau) - \min_{\tau\in[t-T_w,t)} y_p(\tau), \end{aligned} \tag{26}$$

for all $t \geq T_w$.

5.3. Constrained optimization problem

From simulation, steady-state input–output relations between the L2D-setpoints u:

$$u := \begin{bmatrix} \text{L2D}_y\text{-setpoint} & \text{L2D}_z\text{-setpoint} \end{bmatrix}^\top, \tag{27}$$

(1) the average EUV intensity y, (2) the maximum back-reflection $\tilde{z}_1$, and (3) the peak-to-peak variations in EUV intensity $\tilde{z}_2$, denoted by $Q(u)$, $\tilde{G}_1(u)$, and $\tilde{G}_2(u)$, can be obtained, and are shown in Figs. 5(a), 5(b), 5(c), respectively. Knowledge of these mappings is not exploited in the remainder of this section, and is presented merely for verification purposes.

From Fig. 5(a) it can be seen that a maximum average EUV intensity is achievable when the L2D-setpoints in y- and z-direction are around zero. In the case when the L2D-setpoints are zero, the maximum back-reflection signal exceeds 0.8, causing excessive damage to the LPP source. This excessive damage can be prevented by keeping the back-reflection signal below a value of $\gamma_{back} = 0.8$. In addition, the peak-to-peak EUV intensity variation is required to remain below $\gamma_{pp} = 0.28$ which guarantees stable EUV light generation for usage in the lithography scanner. To achieve this goal, we formulate the following constrained optimization problem for the LPP source system:

$$\max_{u\in\mathcal{T}} Q(u) \text{ s.t. } G(u) := \begin{bmatrix} \tilde{G}_1(u) - \gamma_{back} \\ \tilde{G}_2(u) - \gamma_{pp} \end{bmatrix} \leq 0, \tag{28}$$

with $\mathcal{T} := \{u \in \Omega : G(u) \leq 0\}$, and Ω denoting the physical range of the laser-to-droplet position. We assume no knowledge of $Q(u)$ and $G(u)$, and we obtain information on performance and constraint satisfaction only through periodically sampling the outputs $y(t)$ and $z(t)$, where the output $z(t)$ is defined as follows:

$$z(t) := \begin{bmatrix} \tilde{z}_1(t) - \gamma_{back} & \tilde{z}_2(t) - \gamma_{pp} \end{bmatrix}^\top. \tag{29}$$

5.4. Gradient-based sampled-data extremum-seeking algorithm with barrier functions

To solve the constrained optimization problem in (28), we transform the problem to an unconstrained optimization problem by using logarithmic barrier functions $B(u, \mu)$. The resulting unconstrained optimization problem reads

$$\max_{u\in\mathcal{T}^o} \tilde{Q}(u, \mu) := Q(u) - B(u, \mu), \tag{30}$$

with $\tilde{Q}$ the modified objective function, and $\mathcal{T}^o$ denoting the interior of the admissible set $\mathcal{T} = \{u \in \Omega \mid G(u) \leq 0\}$. We employ an extremum-seeking algorithm such as described in Algorithm 1, in which we utilize a gradient-based optimization algorithm. The algorithm exploits an estimate of the gradient of the to-be-optimized modified objective function, determined through a central difference computation, and for which we need to perform $n_v = 4$ experiments for each update of the optimization algorithm. A waiting time $T = 2$ s is chosen, and $T_w = 2$ s is chosen in (26).

The gradient-based optimization algorithm F in (15) is given as follows:

$$F(u, \tilde{Y}(u), \tilde{Z}(u)) := u + \lambda\nabla\tilde{Q}(u, \mu), \tag{31}$$

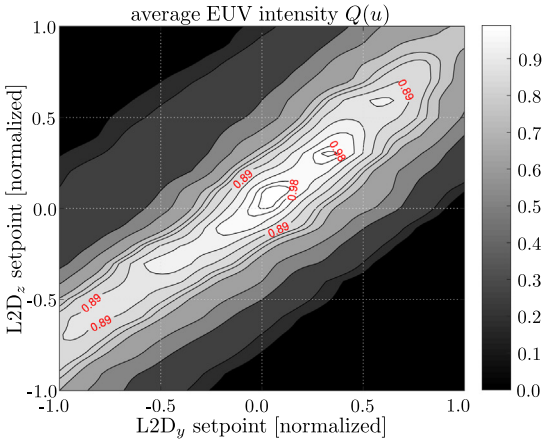

(a) L2D-setpoints to average EUV intensity.

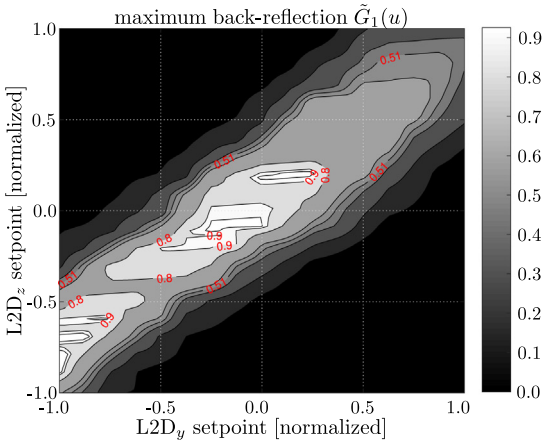

(b) L2D-setpoints to maximum back-reflection.

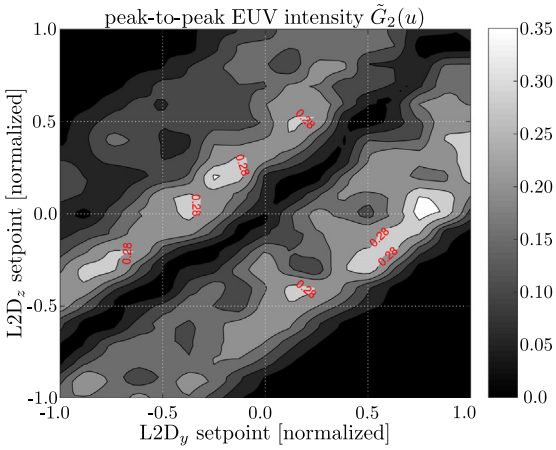

(c) L2D-setpoints to peak-to-peak EUV variation.

Fig. 5. Steady-state input–output mappings.

with so-called optimizer gain λ, and where $\nabla\tilde{Q}(u, \mu)$ denotes the gradient of the modified objective function $\tilde{Q}(u, \mu)$. The actual gradient is unknown since the modified objective function is not analytically known. The gradient is estimated based on the functions $\tilde{Y}(u)$ and $\tilde{Z}(u)$, containing the collected output measurements, and through a central difference computation as follows:

$$\nabla\tilde{Q}(u, \mu) := \frac{1}{2c_v}\begin{bmatrix} 1 & -1 & 0 & 0 \\ 0 & 0 & 1 & -1 \end{bmatrix}\hat{\tilde{Q}}(u, \mu), \tag{32}$$

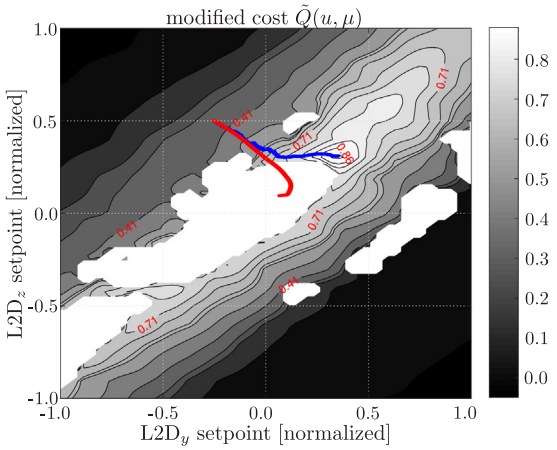

Fig. 6. The modified objective function $\tilde{Q}$, and the evolution of the laser setpoint position in y- and z-direction in the cases $\mu = 0.0$ (red) and $\mu = 0.03$ (blue), respectively without consideration of the constraints on z and with consideration of the constraints on z. The white areas indicate regions where $\tilde{Q}$ is undefined (i.e., outside the set of constraint satisfaction). (For interpretation of the references to color in this figure legend, the reader is referred to the web version of this article.)

with so-called step size c_v, and the measured modified objective function $\hat{\tilde{Q}}(u,\mu) := \tilde{Y}(u) - B(u,\mu)$, with $\tilde{Y}(u)$ as in (16), and the barrier function $B(u,\mu)$ defined as follows:

$$B(u,\mu) := -\mu \left[\sum_{j=1}^{2} \log(-\tilde{Z}_{1j}(u)) \ \cdots \sum_{j=1}^{2} \log(-\tilde{Z}_{4j}(u)) \right]^{\top}, \qquad (33)$$

with $\mu \in \mathbb{R}_{>0}$ the so-called barrier parameter, and where $\tilde{Z}_{ij}$ denotes the ith element from the jth column of the function $\tilde{Z}(u)$ in (16). To facilitate the estimation of the gradient through measurements, the dither functions are chosen as follows: $v_1^{\top} := [c_v \ 0]$, $v_2^{\top} := [-c_v \ 0]$, $v_3^{\top} := [0 \ c_v]$, and $v_4^{\top} = [0 \ -c_v]$.

For illustration purposes only, the modified objective function $\tilde{Q}(u,\mu)$ using barrier functions is visualized in Fig. 6, with $\mu = 0.03$.

Remark 18. In this ESC context, gradient estimation locally around u on the basis of a central difference computation requires the sequential evaluation of the system outputs for inputs $u - c_v$ and $u + c_v$, in which $\pm c_v$ are user-defined and small-valued directional perturbations. However, other optimization methods and dither functions can be used as well. For example, stochastic approximation methods, such as the simultaneous perturbation stochastic approximation algorithm (see Spall, 1997) or the persistently exciting finite differences algorithm (see Teel, 2000b) can be employed as well. Within these algorithms, an estimate of the gradient of the (modified) cost function near the input u is typically obtained on the basis of an excitation with zero-mean random variables.

5.5. Simulation results

To obtain the results presented here, we have used the following numerical values for the algorithm: step-size $c_v = 0.005$ [normalized], optimizer gain $\lambda = \begin{bmatrix} 2 \cdot 10^{-12} & 0 \\ 0 & 2 \cdot 10^{-10} \end{bmatrix}$, and initial L2D-setpoint $u_0 = [-0.25 \ \ 0.5]^{\top}$ [normalized]. Fig. 7 shows the evolution of the laser-to-droplet setpoint position in y- and z-direction as a function of the sampling index, and the corresponding outputs that reflect (1) the average EUV intensity,

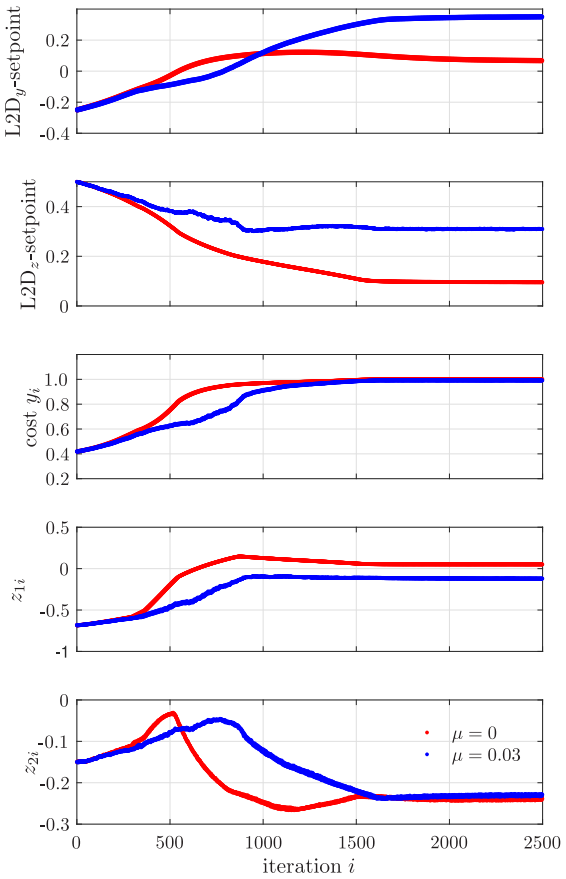

Fig. 7. Evolution of the laser setpoint position in y- and z-direction as a function of the sampling index, and the corresponding average EUV intensity, maximum back-reflection, and peak-to-peak EUV intensity. In the case when $\mu = 0.0$, constraint violation occurs. In the case when $\mu = 0.03$, the average EUV intensity is similarly optimized, however the imposed constraints are satisfied. (For interpretation of the references to color in this figure legend, the reader is referred to the web version of this article.)

(2) the maximum back-reflection, and (3) the peak-to-peak EUV intensity. In particular, Fig. 7 shows iteration-domain results in the unconstrained optimization case ($\mu = 0.0$), and the constrained optimization case ($\mu = 0.03$), and Fig. 6 shows the corresponding trajectories in the input space.

In the case when $\mu = 0.0$, constraint violation occurs. In particular, the optimal operating conditions obtained with the extremum-seeking algorithm and $\mu = 0.0$, leading to an average EUV intensity of approximately 1, violate the constraint on the maximum back-reflection signal γ_{back}. This can be seen by the red plots in Fig. 6 and the fourth sub-figure in Fig. 7. In the case when $\mu = 0.03$, the average EUV intensity achieved is approximately 1 as well, and the constraint on the maximum back-reflection signal is satisfied. This can be seen by the blue plots in Figs. 6 and 7. In both cases, the constraint on the peak-to-peak EUV intensity is satisfied.

Remark 19. Note that, given the non-convexity of the modified cost function $\tilde{Q}(u,\mu)$, see Fig. 6, and given the fact that we employ a gradient-based extremum-seeking algorithm, convergence to the global optimum is not guaranteed. In particular, Assumptions 3 and 7 are, strictly speaking, not satisfied. Namely, the set of actual constrained minimizers $\mathcal{C}_{\mathcal{T}}$ and approximate constrained minimizers $\tilde{\mathcal{C}}_{\mathcal{T}}$ for our modified constrained optimization problem are not compact and the modified cost $\tilde{Q}(u,\mu)$ to-be optimized contains both local and global minima, see, e.g., Fig. 6.

Nevertheless, *locally* (i.e., within a subset of the admissible set $\mathcal{T}$, e.g., a small neighborhood around the approximate constrained global minimizer as visible in Fig. 6) the modified cost $\tilde{Q}(u,\mu)$ is (near) convex. Within that subset the use of a gradient-based optimization algorithm renders Assumption 7 satisfied. Moreover, in practice the gradient-based extremum-seeking algorithm can be used successfully when starting close to the global minimizer or in combination with a multi-start routine as part of a calibration procedure.

6. Conclusion

We have proposed a sampled-data extremum-seeking framework for constrained optimization of dynamical systems using barrier function methods, where both the to-be-optimized objective function and the constraint functions are available through output measurements only. We have shown that for the interconnection of a class of dynamical systems and a class of optimization algorithms, given a sufficiently long waiting time and parameter initialization well within the admissible set, (1) steady-state constraint satisfaction is achieved, and (2) the closed loop is practically asymptotically stable. Finally, we have demonstrated the proposed approach by means of a representative industrial simulation study of the constrained optimization of EUV light generation in an LPP source.

Acknowledgments

The authors gratefully acknowledge Jeroen van de Wijdeven for his contribution to the industrial case study.

Appendix A. Proof of Lemma 12

The proof of Lemma 12 exploits the line of reasoning of the proof of Theorem 1 in Teel and Popović (2001). From Assumption 2 we have that, for any $\epsilon_1, \epsilon_2, \Delta_{\mathcal{X}_0} \in \mathbb{R}_{>0}$, there exist a waiting time $T > 0$ such that

$$\|x(t,x_0,u)\|_{\mathcal{A}(u)} \leq \epsilon_1 \|x_0\|_{\mathcal{A}(u)} + \epsilon_2, \tag{A.1}$$

for all $t \geq T$, all $u \in \mathcal{T}$, and all $\|x_0\|_{\mathcal{A}(u)} \leq \Delta_{\mathcal{X}_0}$. Consider an arbitrary system state x_i with sampling index i during some sequence of inputs k, with algorithm state u_k. Without loss of generality, take $k = 0$. For any $i = 1, \dots, n_v$, with n_v the number of experiments for one algorithm index update, and waiting time $T^* > T$, we have

$$\|x_i\|_{\mathcal{A}(u_0+v_i(u_0))} \leq \epsilon_1 \|x_{i-1}\|_{\mathcal{A}(u_0+v_i(u_0))} + \epsilon_2, \tag{A.2}$$

for $\|x_{i-1}\|_{\mathcal{A}(u_0+v_i(u_0))} \leq \Delta_{\mathcal{X}_0}$, with the state $x_i := x(T^*, x_{i-1}, u_0 + v_i(u_0))$. From item 2 of Assumption 11 it follows that for any $\Delta_{\mathcal{U}} > 0$ there exists a constant $L_{\mathcal{A}} \in \mathbb{R}_{>0}$ such that we have the following inequality:

$$\begin{aligned}\mathcal{A}(u_0 + v_i(u_0)) \subseteq \mathcal{A}(u_0 + v_{i-1}(u_0)) \\ + L_{\mathcal{A}} \|v_i(u_0) - v_{i-1}(u_0)\| \overline{\mathcal{B}},\end{aligned} \tag{A.3}$$

with $\max\{\|u_0 + v_i(u_0)\|_{\tilde{\mathcal{C}}_{\mathcal{T}}}, \|u_0 + v_{i-1}(u_0)\|_{\tilde{\mathcal{C}}_{\mathcal{T}}}\} \leq \Delta_{\mathcal{U}}$ for $i = 1, \dots, n_v$, and with $v_0(\cdot) := v_{n_v}(\cdot)$ (as defined in Lemma 12). From Lemma 1 in Teel and Popović (2001) and (A.3), we obtain the following inequality:

$$\begin{aligned}\|x_{i-1}\|_{\mathcal{A}(u_0+v_i(u_0))} \leq \|x_{i-1}\|_{\mathcal{A}(u_0+v_{i-1}(u_0))} \\ + L_{\mathcal{A}} \|v_i(u_0) - v_{i-1}(u_0)\|.\end{aligned} \tag{A.4}$$

Combining (A.4) and (A.2), and by using item 4 of Assumption 11, for any input $u \in \bar{\mathcal{T}}$ with $\bar{\mathcal{T}}$ an arbitrary (large) strict subset of $\mathcal{T}^o$ and $\|u\|_{\tilde{\mathcal{C}}_{\mathcal{T}}} \leq \Delta_{\mathcal{U}}$, and any $i = 1, \dots, n_v$, we obtain the following inequality:

$$\begin{aligned}\|x_i\|_{\mathcal{A}(u_0+v_i(u_0))} \leq \epsilon_1 \big(\|x_{i-1}\|_{\mathcal{A}(u_0+v_{i-1}(u_0))} \\ + L_{\mathcal{A}} \|v_i(u_0) - v_{i-1}(u_0)\| \big) + \epsilon_2,\end{aligned} \tag{A.5}$$

for $\|x_{i-1}\|_{\mathcal{A}(u_0+v_{i-1}(u_0))} \leq \Delta_{\mathcal{X}_0} - 2L_{\mathcal{A}}(M_v \Delta_{\mathcal{U}} + c_v)$, such that $\|x_{i-1}\|_{\mathcal{A}(u+v_i(u))} \leq \Delta_{\mathcal{X}_0}$, and with $v_0(\cdot) := v_{n_v}(\cdot)$. Now, let us determine the distance of the system state x_{n_v} to the attractor $\mathcal{A}(u_0 + v_{n_v}(u_0))$ at the end of the current sequence of inputs, as a function of the distance of the state x_0 to $\mathcal{A}(u_0 + v_{n_v}(u_0))$ at the beginning of the current sequence of inputs (i.e., end of the previous sequence of inputs), with $\|x_0\|_{\mathcal{A}(u_0+v_{n_v}(u_0))} \leq \Delta_{\mathcal{X}}$:

$$\begin{aligned}\|x_i\|_{\mathcal{A}(u_0+v_i(u_0))} \leq \epsilon_1 \Bigg(\epsilon_1^{i-1} \|x_0\|_{\mathcal{A}(u_0+v_{n_v}(u_0))} \\ + L_{\mathcal{A}} \sum_{j=1}^{i} (\epsilon_1^{i-j} \|v_j(u_0) - v_{j-1}(u_0)\|) \Bigg) + \epsilon_2 \sum_{j=1}^{i} \epsilon_1^{i-j},\end{aligned} \tag{A.6}$$

for all $i = 1, \dots, n_v$ and with $v_0(\cdot) := v_{n_v}(\cdot)$. By considering $\epsilon_1 \in (0, 1]$, which can be accomplished by having a sufficiently long waiting time T, see, e.g., Assumption 2, we obtain the following inequality:

$$\begin{aligned}\|x_i\|_{\mathcal{A}(u_0+v_i(u_0))} \leq \epsilon_1 \Bigg(\|x_0\|_{\mathcal{A}(u_0+v_{n_v}(u_0))} \\ + L_{\mathcal{A}} \sum_{j=1}^{i} (\|v_j(u_0) - v_{j-1}(u_0)\|) \Bigg) + n_v \epsilon_2,\end{aligned} \tag{A.7}$$

for all $i = 1, \dots, n_v$, and with $v_0(\cdot) := v_{n_v}(\cdot)$. Define $\bar{x} := x_0$ the state of the plant at the beginning of the current sequence of inputs, and $\bar{x}^+ := x_{n_v}$ the new state of the plant at the end of the current sequence of inputs. Moreover, let $u := u_0$ be the current state of the algorithm. From (A.7) and for $i = n_v$, for any $\Delta_{\mathcal{X}}, \Delta_{\mathcal{U}}, \epsilon_2 \in \mathbb{R}_{>0}$ and $\epsilon_1 \in (0, 1]$, there exists a sufficiently long waiting time $T^* \geq T$ such that for any $\bar{x} \in \mathcal{X}$ with $\|\bar{x}\|_{\mathcal{A}(u+v_{n_v}(u))} \leq \Delta_{\mathcal{X}}$, and any $u \in \bar{\mathcal{T}}$ with $\bar{\mathcal{T}}$ an arbitrary (large) strict subset of $\mathcal{T}^o$ and with $\|u\|_{\tilde{\mathcal{C}}_{\mathcal{T}}} \leq \Delta_{\mathcal{U}}$, we can write the following inequality:

$$\begin{aligned}\bar{x}^+ \in \mathcal{A}(u + v_{n_v}(u)) + \Bigg(\epsilon_1 \Bigg(\|\bar{x}\|_{\mathcal{A}(u+v_{n_v}(u))} \\ + L_{\mathcal{A}} \sum_{j=1}^{n_v} \|v_j(u) - v_{j-1}(u)\| \Bigg) + n_v \epsilon_2 \Bigg) \overline{\mathcal{B}},\end{aligned} \tag{A.8}$$

with $v_0(\cdot) := v_{n_v}(\cdot)$. This concludes the proof of Lemma 12. □

Appendix B. Proof of Theorem 13

The structure of the proof is as follows. First, a bound on $\Delta V_{\Sigma}(u)$ is derived. Second, a bound on $\Delta V_{\Sigma_p}(\psi, \bar{x})$ is derived. Third, a bound on $\Delta W(\psi, \bar{x}, u)$ is derived. Fourth, we show (1) constraint satisfaction and (2) the convergence of u to a region around the set of approximate minimizers $\tilde{\mathcal{C}}_{\mathcal{T}}$.

Step 1: Let us derive a bound on $\Delta V_{\Sigma}(u) := V_{\Sigma}(u^+) - V_{\Sigma}(u)$, where u^+ is generated by (21) in Lemma 12, i.e., $u^+ \in F(u, \tilde{Y}(u), \tilde{Z}(u))$. Let $\tilde{u} \in F(u, Y(u), Z(u))$ be the closest point to $u^+ \in F(u, \tilde{Y}(u), \tilde{Z}(u))$. From Assumption 7, it follows that for any $u \in \bar{\mathcal{T}}$ with $\bar{\mathcal{T}}$ an arbitrary (large) strict subset of $\mathcal{T}^o$, there exist constants $L_V \in \mathbb{R}_{>0}$ and $\delta \in \mathbb{R}_{\geq 0}$, and a $\mathcal{K}_{\infty}$-function $\rho(\cdot)$, such that we can write

$$\begin{aligned}\Delta V_{\Sigma}(u) = V_{\Sigma}(u^+) - V_{\Sigma}(u) \\ \leq L_V \|u^+ - \tilde{u}\| - \rho(V_{\Sigma}(u)) + \delta.\end{aligned} \tag{B.1}$$

From Assumption 11, it follows that

$$\|u^+ - \tilde{u}\| \leq L_Y \|\tilde{Y}(u) - Y(u)\| + L_Z \|\tilde{Z}(u) - Z(u)\|, \tag{B.2}$$

which, together with (B.1), leads to the following inequality:

$$\begin{aligned}\Delta V_\Sigma(u) &\le L_V L_Y \|\tilde{Y}(u) - Y(u)\| \\ &+ L_V L_Z \|\tilde{Z}(u) - Z(u)\| - \rho(V_\Sigma(u)) + \delta.\end{aligned} \tag{B.3}$$

From Assumption 11 and after one sequence of inputs it also follows that

$$\begin{aligned}\|\tilde{Y}(u) - Y(u)\| &\le n_v L_H \|\bar{x}^+\|_{\mathcal{A}(u+v_{n_v}(u))}, \\ \|\tilde{Z}(u) - Z(u)\| &\le n_v L_G \|\bar{x}^+\|_{\mathcal{A}(u+v_{n_v}(u))}.\end{aligned} \tag{B.4}$$

Let us define $\tilde{L} := n_v L_V (L_Y L_H + L_Z L_G)$. As such, from (B.3)–(B.4) we obtain the following inequality:

$$\Delta V_\Sigma(u) \le \tilde{L} \|\bar{x}^+\|_{\mathcal{A}(u+v_{n_v}(u))} - \rho(V_\Sigma(u)) + \delta. \tag{B.5}$$

Step 2: Let us derive a bound on $\Delta V_{\Sigma_p}(\psi, \bar{x}) := V_{\Sigma_p}(\psi^+, \bar{x}^+) - V_{\Sigma_p}(\psi, \bar{x})$. Since $V_{\Sigma_p}(\psi, \bar{x}) := \sigma \|\psi\|_{\tilde{\mathcal{C}}_\mathcal{T}} + \|\bar{x}\|_{\mathcal{A}(\psi+v_{n_v}(\psi))}$ with $\sigma \in \mathbb{R}_{>0}$, we obtain the following equation:

$$\begin{aligned}\Delta V_{\Sigma_p}(\psi, \bar{x}) = \|\bar{x}^+\|_{\mathcal{A}(u+v_{n_v}(u))} - \|\bar{x}\|_{\mathcal{A}(\psi+v_{n_v}(\psi))} \\ + \sigma \|u\|_{\tilde{\mathcal{C}}_\mathcal{T}} - \sigma \|\psi\|_{\tilde{\mathcal{C}}_\mathcal{T}},\end{aligned} \tag{B.6}$$

where we used that $\psi^+ = u$.

Step 3: From (B.5) and (B.6) and $W(\psi, \bar{x}, u)$ in (22), it follows that

$$\begin{aligned}\Delta W(\psi, \bar{x}, u) &= \Delta V_{\Sigma_p}(\psi, \bar{x}) + 2\Delta V_\Sigma(u) \\ &\le \bar{L} \|\bar{x}^+\|_{\mathcal{A}(u+v_{n_v}(u))} - \|\bar{x}\|_{\mathcal{A}(\psi+v_{n_v}(\psi))} \\ &+ \sigma \|u\|_{\tilde{\mathcal{C}}_\mathcal{T}} - \sigma \|\psi\|_{\tilde{\mathcal{C}}_\mathcal{T}} - 2\rho(V_\Sigma(u)) + 2\delta,\end{aligned} \tag{B.7}$$

with $\bar{L} := 1 + 2\tilde{L}$. By using Lemma 12 and (20) in Assumption 11, we obtain the following inequality:

$$\begin{aligned}\Delta W(\psi, \bar{x}, u) &\le \bar{L}\epsilon_1 \big(\|\bar{x}\|_{\mathcal{A}(u+v_{n_v}(u))} - \|\bar{x}\|_{\mathcal{A}(\psi+v_{n_v}(\psi))} \big) \\ &+ (\sigma + 2\bar{L}\epsilon_1 L_\mathcal{A} n_v M_v) \|u\|_{\tilde{\mathcal{C}}_\mathcal{T}} + 2\bar{L}\epsilon_1 L_\mathcal{A} n_v c_v \\ &+ \bar{L} n_v \epsilon_2 - (1 - \bar{L}\epsilon_1) \|\bar{x}\|_{\mathcal{A}(\psi+v_{n_v}(\psi))} \\ &- \sigma \|\psi\|_{\tilde{\mathcal{C}}_\mathcal{T}} - 2\rho(V_\Sigma(u)) + 2\delta,\end{aligned} \tag{B.8}$$

From Lemmas 1 and 2 in Teel and Popović (2001), there exists a $\kappa \in \mathbb{R}_{\ge 0}$ such that we obtain the following inequality:

$$\begin{aligned}&\|\bar{x}\|_{\mathcal{A}(u+v_{n_v}(u))} - \|\bar{x}\|_{\mathcal{A}(\psi+v_{n_v}(\psi))} \\ &\le L_\mathcal{A} \Big((1 + M_v) \|u\|_{\tilde{\mathcal{C}}_\mathcal{T}} + (1 + M_v) \|\psi\|_{\tilde{\mathcal{C}}_\mathcal{T}} + 2c_v + \kappa \Big).\end{aligned} \tag{B.9}$$

From substitution of (B.9) into (B.8), and using Assumption 7, we obtain the following inequality:

$$\begin{aligned}\Delta W(\psi, \bar{x}, u) &\le -(\sigma - \bar{L}\epsilon_1 L_\mathcal{A}(1 + M_v)) \|\psi\|_{\tilde{\mathcal{C}}_\mathcal{T}} \\ &+ 2\bar{L}\epsilon_1 L_\mathcal{A} c_v + \bar{L}\epsilon_1 L_\mathcal{A} \kappa + 2\bar{L}\epsilon_1 L_\mathcal{A} n_v c_v + \bar{L} n_v \epsilon_2 \\ &+ (\sigma + \bar{L}\epsilon_1 L_\mathcal{A}(2n_v M_v + 1 + M_v)) \|u\|_{\tilde{\mathcal{C}}_\mathcal{T}} \\ &- (1 - \bar{L}\epsilon_1) \|\bar{x}\|_{\mathcal{A}(\psi+v_{n_v}(\psi))} - 2\rho(V_\Sigma(u)) + 2\delta.\end{aligned} \tag{B.10}$$

For any (arbitrarily small) $\gamma \in \mathbb{R}_{\ge 0}$, we ensure that $2\bar{L}\epsilon_1 L_\mathcal{A} c_v + \bar{L}\epsilon_1 L_\mathcal{A} \kappa \le \frac{1}{2}\gamma$ and $2\bar{L}\epsilon_1 L_\mathcal{A} n_v c_v + \bar{L} n_v \epsilon_2 \le \frac{1}{2}\gamma$ by designing $\epsilon_1 \in (0, 1]$ and $\epsilon_2 \in \mathbb{R}_{>0}$ sufficiently small, which can be achieved by selecting a sufficiently long waiting time T, see the last item of Assumption 2. As such, we obtain the following inequality:

$$\begin{aligned}\Delta W(\psi, \bar{x}, u) &\le -(\sigma - \bar{L}\epsilon_1 L_\mathcal{A}(1 + M_v)) \|\psi\|_{\tilde{\mathcal{C}}_\mathcal{T}} \\ &+ (\sigma + \bar{L}\epsilon_1 L_\mathcal{A}(2n_v M_v + 1 + M_v)) \|u\|_{\tilde{\mathcal{C}}_\mathcal{T}} \\ &- (1 - \bar{L}\epsilon_1) \|\bar{x}\|_{\mathcal{A}(\psi+v_{n_v}(\psi))} - 2\rho(V_\Sigma(u)) + 2\delta + \gamma.\end{aligned} \tag{B.11}$$

Moreover, for any $\sigma \in \mathbb{R}_{>0}$, we ensure that $\bar{L}\epsilon_1 \le \frac{1}{2}$, $\bar{L}\epsilon_1 L_\mathcal{A}(1 + M_v) \le \frac{1}{2}\sigma$, and $2\bar{L}\epsilon_1 L_\mathcal{A} n_v M_v \le \frac{1}{2}\sigma$ by designing $\epsilon_1 \in (0, 1]$ sufficiently small. This can be achieved by selecting a sufficiently long waiting time T, see the last item of Assumption 2. This leads to the following inequality:

$$\begin{aligned}\Delta W(\psi, \bar{x}, u) &\le -\frac{1}{2} \|\bar{x}\|_{\mathcal{A}(\psi+v_{n_v}(\psi))} - \frac{1}{2}\sigma \|\psi\|_{\tilde{\mathcal{C}}_\mathcal{T}} \\ &+ 2\sigma \|u\|_{\tilde{\mathcal{C}}_\mathcal{T}} - 2\rho(V_\Sigma(u)) + 2\delta + \gamma.\end{aligned} \tag{B.12}$$

Let us define a $\mathcal{K}_\infty$-function $\bar{\gamma}(\cdot) := \min\{\rho(\cdot), \mathrm{id}(\cdot)\}$. This implies that $\bar{\gamma}(\cdot) \le \rho(\cdot)$, and $\bar{\gamma}(\cdot) \le \mathrm{id}(\cdot)$. As such, $-\frac{1}{2}V_{\Sigma_p}(\psi, \bar{x}) \le -\bar{\gamma}(\frac{1}{2}V_{\Sigma_p}(\psi, \bar{x}))$, and $-\rho(V_\Sigma(u)) \le -\bar{\gamma}(V_\Sigma(u))$. Moreover, given the fact that $\bar{\gamma}(\cdot) \in \mathcal{K}_\infty$, it follows that $\bar{\gamma}\left(\frac{1}{2}(\frac{1}{2}V_{\Sigma_p}(\psi, \bar{x}) + V_\Sigma(u))\right) \le \bar{\gamma}\left(\frac{1}{2}V_{\Sigma_p}(\psi, \bar{x})\right) + \bar{\gamma}(V_\Sigma(u))$ (see, e.g., Kellett (2014)). With $V_{\Sigma_p}(\psi, \bar{x}) := \sigma \|\psi\|_{\tilde{\mathcal{C}}_\mathcal{T}} + \|\bar{x}\|_{\mathcal{A}(\psi+v_{n_v}(\psi))}$, (B.12) results in the following inequality:

$$\begin{aligned}\Delta W(\psi, \bar{x}, u) &\le -\bar{\gamma}\left(\frac{1}{4}(V_{\Sigma_p}(\psi, \bar{x}) + 2V_\Sigma(u))\right) \\ &+ 2\sigma \|u\|_{\tilde{\mathcal{C}}_\mathcal{T}} - \rho(V_\Sigma(u)) + 2\delta + \gamma,\end{aligned} \tag{B.13}$$

Let us define a function $\tilde{\gamma}(\cdot) \in \mathcal{K}_\infty$ such that

$$\tilde{\gamma}\left(V_{\Sigma_p}(\psi, \bar{x}) + 2V_\Sigma(u)\right) := \bar{\gamma}\left(\frac{1}{4}\left(V_{\Sigma_p}(\psi, \bar{x}) + 2V_\Sigma(u)\right)\right). \tag{B.14}$$

From item 2 in Assumption 7, we have that there exists a function $\alpha \in \mathcal{K}_\infty$ such that $\alpha(\|u\|_{\tilde{\mathcal{C}}_\mathcal{T}}) \le V_\Sigma(u)$. From this fact and $\rho \in \mathcal{K}_\infty$, we obtain that $-\rho(V_\Sigma(u)) \le -\rho(\alpha(\|u\|_{\tilde{\mathcal{C}}_\mathcal{T}}))$. For any $\alpha, \rho \in \mathcal{K}_\infty$, we have that $\tilde{\rho}(\cdot) := \rho(\alpha(\cdot)) \in \mathcal{K}_\infty$, which implies that $-\rho(V_\Sigma(u)) \le -\tilde{\rho}(\|u\|_{\tilde{\mathcal{C}}_\mathcal{T}})$. For any $\Delta_\mathcal{U} \in \mathbb{R}_{>0}$ and any small $\delta_V \in \mathbb{R}_{>0}$, there exists a $c \in \mathbb{R}_{>0}$ such that $-\tilde{\rho}(\|u\|_{\tilde{\mathcal{C}}_\mathcal{T}}) \le -c\|u\|_{\tilde{\mathcal{C}}_\mathcal{T}} + \delta_V$ for $u \in \bar{\mathcal{T}}$ and with $\|u\|_{\tilde{\mathcal{C}}_\mathcal{T}} \le \Delta_\mathcal{U}$. From (B.14), (22), and $\sigma := \frac{c}{2}$, we obtain the following inequality:

$$\Delta W(\psi, \bar{x}, u) \le -\tilde{\gamma}(W(\psi, \bar{x}, u)) + 2\delta + \gamma + \delta_V, \tag{B.15}$$

with any small $\delta_V \in \mathbb{R}_{>0}$.

Step 4: Next, we will use the inequality in (B.15) to (1) show constraint satisfaction and (2) the convergence of u to a neighborhood of the set of approximate minimizers $\tilde{\mathcal{C}}_\mathcal{T}$. Let $\hat{\rho} \in \mathcal{K}_\infty$ such that $(\mathrm{id} - \hat{\rho}) \in \mathcal{K}_\infty$. For any $\hat{\rho} \circ \tilde{\gamma}(W(\psi, \bar{x}, u)) \ge 2\delta + \gamma + \delta_V$ we obtain that

$$\Delta W(\psi, \bar{x}, u) \le -(\mathrm{id} - \hat{\rho}) \circ \tilde{\gamma}(W(\psi, \bar{x}, u)). \tag{B.16}$$

From (B.16) and the comparison lemma, see, e.g., Lemma 4.3 in Jiang and Wang (2002), we have that there exists some $\mathcal{KL}$-function $\hat{\beta}$ such that

$$\begin{aligned}W(\psi_k, \bar{x}_k, u_k) \le \max\{&\hat{\beta}(W(\psi_0, \bar{x}_0, u_0), k), \\ &\tilde{\gamma}^{-1} \circ \hat{\rho}^{-1}(2\delta + \gamma + \delta_V)\},\end{aligned} \tag{B.17}$$

for all $k \in \mathbb{N}$. This shows the validity of inequality (25) in the theorem. Based on this inequality we can now validate the two statements in the theorem on constraint satisfaction and the convergence to a neighborhood of the approximate constrained minimizer set:

- For any $u_0, \psi_0 \in \mathcal{V} \subset \bar{\mathcal{T}}$ and $\bar{x}_0 \in \mathcal{X}$ with $\|u_0\|_{\tilde{\mathcal{C}}_\mathcal{T}} \le \Delta_\mathcal{U}$, $\|\psi_0\|_{\tilde{\mathcal{C}}_\mathcal{T}} \le \Delta_\mathcal{U}$, and $\|\bar{x}_0\|_{\mathcal{A}(\psi_0+v_{n_v}(\psi_0))} \le \Delta_\mathcal{X}$ with some $\Delta_\mathcal{U}, \Delta_\mathcal{X} \in \mathbb{R}_{\ge 0}$, we have that $W(\psi_0, \bar{x}_0, u_0)$ is bounded, i.e., $W(\psi_0, \bar{x}_0, u_0) \le \Delta_W$ for some $\Delta_W \in \mathbb{R}_{\ge 0}$. From (B.17) we obtain that $W(\psi_k, \bar{x}_k, u_k)$ is bounded for all $k \in \mathbb{N}$. Next, boundedness of $W(\psi_k, \bar{x}_k, u_k)$ for all $k \in \mathbb{N}$ implies that $V_\Sigma(u_k)$ is bounded for all $k \in \mathbb{N}$. As such, from Assumption 7 and boundedness of $V_\Sigma(u_k)$ it follows that $u_k \in \mathcal{T}^o$ for all $k \ge 0$, i.e., steady-state constraints satisfaction is guaranteed for all $k \in \mathbb{N}$.
- From the inequality in (B.17), we have the following ultimate bound for W:

$$\lim_{k \to \infty} W(\psi_k, \bar{x}_k, u_k) = \tilde{\gamma}^{-1} \circ \hat{\rho}^{-1}(2\delta + \gamma + \delta_V). \tag{B.18}$$

Given the fact that $2V_\Sigma(u) \leq W(\psi, \bar{x}, u)$, and $\alpha(\|u\|_{\tilde{\mathcal{C}}_\mathcal{T}}) \leq V_\Sigma(u)$ which follows from item 2 in Assumption 7, we have that the solutions converge to a set $\mathcal{Y}_u := \{u \in \mathcal{T}^o \mid \|u\|_{\tilde{\mathcal{C}}_\mathcal{T}} \leq \alpha^{-1}\big(\frac{1}{2}\tilde{\gamma}^{-1} \circ \hat{\rho}^{-1}(2\delta + \gamma + \delta_V)\big)\}$.

The set $\mathcal{Y}_u$ can be made arbitrarily small. Namely, (1) $\delta_V \in \mathbb{R}_{>0}$ can be any arbitrarily small constant, (2) we can make γ arbitrarily small by choosing a sufficiently large waiting time $T \in \mathbb{R}_{>0}$, and (3) δ, which is defined in Assumption 7, can be made sufficiently small by tuning the parameters of the particular optimization algorithm F, as discussed in Assumption 7 and Remark 9. This completes the proof of Theorem 13. □

References

Atta, K. T., Guay, M., & Lucchese, R. (2019). A geometric phasor extremum seeking control approach with measured constraints. In *Proceedings of the 58th IEEE conference on decision and control, Nice, France* (pp. 1494–1500).

Boyd, S., & Vandenberghe, L. (2009). *Convex optimization* (7th ed.). Cambridge University Press.

DeHaan, D., & Guay, M. (2005). Extremum-seeking control of state-constrained nonlinear systems. *Automatica*, *41*(9), 1567–1574.

Dürr, H.-B., & Ebenbauer, C. (2011). A smooth vector field for saddle point problems. In *Proceedings of the 50th IEEE conference on decision and control, Orlando, USA* (pp. 4654–4660).

Dürr, H.-B., Zeng, C., & Ebenbauer, C. (2013). Saddle point seeking for convex optimization problems. In *9th IFAC symposium on nonlinear control systems, Vol. 46* (pp. 540–545). (23).

Fiacco, A. V., & McCormick, G. P. (1990). Nonlinear programming: sequential unconstrained minimization techniques.

Frihauf, P., Riggs, D. J., Graham, M. R., Chang, S., & Dunstan, W. J. (2013). System and method to optimize extreme ultraviolet light generation. United States Patent, Patent No: US 8598552 B1.

Guay, M., Moshksar, E., & Dochain, D. (2014). A constrained extremum-seeking control approach. *International Journal of Robust and Nonlinear Control*, *25*(16), 3132–3153.

Haring, M., van de Wouw, N., & Nešić, D. (2013). Extremum-seeking control for nonlinear systems with periodic steady-state outputs. *Automatica*, *49*(6), 1883–1891.

Hazeleger, L., Nešić, D., & van de Wouw, N. (2019). Sampled-data extremum-seeking control for optimization of constrained dynamical systems using barrier function methods. In *Proceedings of the 58th conference on decision and control, Nice, France* (pp. 213–219).

Jiang, Z.-P., & Wang, Y. (2002). A converse Lyapunov theorem for discrete-time systems with disturbances. *Systems & Control Letters*, *45*, 49–58.

Kellett, C. M. (2014). A compendium of comparison function results. *Mathematics of Control, Signals, and Systems*, *26*(3), 339–374.

Kellett, C. M. (2015). Classical converse theorems in Lyapunov's second method. *Discrete and Continuous Dynamical Systems. Series B*, *20*(8), 2333–2360.

Kellett, C. M., & Teel, A. R. (2004). Weak converse Lyapunov theorems and control-Lyapunov functions. *SIAM Journal on Control and Optimization*, *42*(6), 1934–1959.

Khong, S. Z., Nešić, D., Manzie, C., & Tan, Y. (2013). Multidimensional global extremum seeking via the DIRECT method. *Automatica*, *49*(7), 1970.

Khong, S. Z., Nešić, D., Tan, Y., & Manzie, C. (2013a). Trajectory-based proofs for sampled-data extremum seeking control. In *Proceedings of the American control conference, Washington, DC* (pp. 2751–2756).

Khong, S. Z., Nešić, D., Tan, Y., & Manzie, C. (2013b). Unified frameworks for sampled-data extremum-seeking control: global optimization and multi-unit systems. *Automatica*, *49*, 2720–2733.

Krstić, M., & Wang, H.-H. (2000). Stability of extremum-seeking feedback for general nonlinear dynamic systems. *Automatica*, *36*(4), 595–601.

Kvaternik, K., & Pavel, L. (2011). Interconnection conditions for the stability of nonlinear sampled-data extremum seeking schemes. In *Proceedings of the 50th IEEE conference on decision and control, Orlando, USA* (pp. 4448–4454).

Labar, C., Garone, E., Kinnaert, M., & Ebenbauer, C. (2019). Constrained extremum seeking: a modified-barrier function approach. *IFAC-PapersOnline*, *52*(16), 694–699, 11th IFAC Symposium on Nonlinear Control Systems NOLCOS 2019.

Liao, C.-K., Manzie, C., Chapman, A., & Alpcan, T. (2019). Constrained extremum seeking of a MIMO dynamic system. *Automatica*, *108*, Article 108496.

Mills, G., & Krstić, M. (2014). Constrained extremum seeking in 1 dimension. In *Proceedings of the 53th conference on decision and control, Los Angeles, USA* (pp. 2654–2659).

Nešić, D., Nguyen, T., Tan, Y., & Manzie, C. (2013). A non-gradient approach to global extremum seeking: An adaptation of the shubert algorithm. *Automatica*, *49*(3), 709–815.

Nešić, D., Teel, A. R., & Kokotović, P. V. (1999). Sufficient conditions for stabilization of sampled-data nonlinear systems via discrete-time approximations. *Systems & Control Letters*, *38*, 259–270.

Ramos, M., Manzie, C., & Shekhar, R. (2017). Online optimisation of fuel consumption subject to NOx constraints. *IFAC-PapersOnLine*, *50*(1), 8901–8906, 20th IFAC World Congress.

Spall, J. C. (1997). A one-measurement form of simultaneous perturbation stochastic approximation. *Automatica*, *33*(1), 109–112.

Srinivasan, B., Biegler, L. T., & Bonvin, D. (2008). Tracking the necessary conditions of optimality with changing set of active constraints using a barrier-penalty function. *Computers and Chemical Engineering*, *32*, 572–579.

Tan, Y., Li, Y., & Mareels, I. M. Y. (2013). Extremum seeking for constrained inputs. *IEEE Transactions on Automatic Control*, *58*(9), 2405–2410.

Tan, Y., Nešić, D., & Mareels, I. (2006). On non-local stability properties of extremum seeking control. *Automatica*, *42*(6), 889–903.

Teel, A. R. (2000). Lyapunov methods in nonsmooth optimization, part I: Quasi-Newton algorithms for Lipschitz, regular functions. In *Proceedings of the 39th conference on decision and control, Sydney, Australia* (pp. 112–117).

Teel, A. R. (2000). Lyapunov methods in nonsmooth optimization, part II: persistently exciting finite differences. In *Proceedings of the 39th conference on decision and control, Sydney, Australia* (pp. 118–123).

Teel, A. R., & Popović, D. (2001). Solving smooth and nonsmooth multivariable extremum seeking problems by the methods of nonlinear programming. In *Proceedings of the American control conference, Arlington, VA* (pp. 25–27).

Teel, A. R., & Praly, L. (2000). A smooth Lyapunov function from a class-KL estimate involving two positive semidefinite functions. *ESAIM: Control, Optimisation and Calculus of Variations*, *5*, 313–368.

van der Weijst, R., van Keulen, T., & Willems, F. (2019). Constrained multivariable extremum-seeking for online fuel-efficiency optimization of diesel engines. *Control Engineering Practice*, *87*, 133–144.

Leroy Hazeleger received his M.Sc.-degree in Systems and Control within the Department of Mechanical Engineering at the Eindhoven University of Technology, The Netherlands, in 2015. He received his Ph.D.-degree within the Dynamics and Control Group at the Eindhoven University of Technology, The Netherlands, in 2020. Currently, Leroy Hazeleger is working as a Mechatronics Engineer at Thermo Fisher Scientific, Eindhoven, The Netherlands.

Dragan Nešić is a Professor at the Department of Electrical and Electronic Engineering at The University of Melbourne. He received his Bachelor of Mechanical Engineering Degree at the University of Belgrade (1990) and his Ph.D. at the Australian National University (1997). His research interests are in the broad area of control engineering including its mathematical foundations (e.g. Lyapunov stability theory, hybrid systems, singular perturbations, averaging) and its applications to various areas of engineering (e.g. automotive control, optical telecommunications) and science (e.g. neuroscience). More specifically, he has made significant contributions to the areas of nonlinear sampled-data systems, nonlinear networked control systems, event-triggered control, optimization-based control and extremum seeking control and he presented several keynote lectures on these topics at international conferences. He is a Fellow of IEEE and a Fellow of IFAC and he served as a Distinguished Lecturer of the Control Systems Society of the IEEE. He was a co-recipient (with M. Nagahara and D. Quevedo) of the George S. Axelby Outstanding Paper Award (2017). He is a recipient of numerous awards and prizes, including Doctorate Honoris Causa by the University of Lorraine (2019), Humboldt Research Award (2020), Humboldt Research Fellowship (2003–2004), as well as Future Fellowship (2010–2014) and an Australian Professorial Fellowship (2004–2009) funded by the Australian Research Council. He is an Associate Editor for the journal IEEE Transactions on Network Control Systems (CONES) and Foundations and Trends in Systems and Control. He has also served as Associate Editor for the IEEE Transactions on Automatic Control, Automatica, European Journal of Control and Systems and Control Letters. He was a General Co-Chair of 2017 IEEE Conference on Decision and Control and a General Chair of the 2011 Australian Control Conference. He served on International Program Committees of many international conferences, such as the American Control Conference, IEEE Conference on Decision and Control, NOLCOS, Asian Control Conference, and European Control Conference. He also served on various committees including the Board of Governors, IEEE Control Systems Society.

Nathan van de Wouw, (born, 1970) obtained his M.Sc.-degree (with honors) and Ph.D.-degree in Mechanical Engineering from the Eindhoven University of Technology, Eindhoven, the Netherlands, in 1994 and 1999, respectively. He currently holds a full professor position at the Mechanical Engineering Department of the Eindhoven University of Technology, The Netherlands. Nathan van de Wouw also holds an adjunct full professor position at the University of Minnesota, U.S.A. In 2000, Nathan van de Wouw has been working at Philips Applied Technologies, Eindhoven, The Netherlands, and, in 2001, he has been working at the Netherlands Organisation for Applied Scientific Research (TNO), Delft, The Netherlands. He has held positions as a visiting professor at the University of California Santa Barbara, U.S.A., in 2006/2007, at the University of Melbourne, Australia, in 2009/2010 and at the University of Minnesota, U.S.A., in 2012 and 2013. He has held a (part-time) full professor position the Delft University of Technology, the Netherlands, from 2015–2019. He has published the books 'Uniform Output Regulation of Nonlinear Systems: A convergent Dynamics Approach' with A.V. Pavlov and H. Nijmeijer (Birkhauser, 2005) and 'Stability and Convergence of Mechanical Systems with Unilateral Constraints' with R.I. Leine (Springer-Verlag, 2008). He currently is an Associate Editor for the journals "Automatica" and "IEEE Transactions on Control Systems Technology". In 2015, he received the IEEE Control Systems Technology Award "For the development and application of variable-gain control techniques for high-performance motion systems". His current research interests are the modeling, model reduction, analysis and control of nonlinear/hybrid and delay systems, with applications to vehicular platooning, high-tech systems, resource exploration, smart energy systems and networked control systems.